Chapter 9

Relationship between Land Use and Water Quality and its Assessment Using Hyperspectral Remote Sensing in Mid-Atlantic Estuaries

Gulnihal Ozbay, Chunlei Fan and Zhiming Yang

Additional information is available at the end of the chapter

http://dx.doi.org/10.5772/66620

Abstract

Mid-Atlantic coastal waters are under increasing pressures from anthropogenic disturbances at various temporal and spatial scales exacerbated by the climate change. According to the National Oceanic Atmospheric Association (NOAA), 10 of the 22 estuaries in the Mid-Atlantic, including the Chesapeake Bay, exhibit high levels of eutrophic conditions while seven, including Delaware Bay, exhibit low conditions. Chesapeake Bay is the largest estuarine system in the United States and undergoes frequent eutrophication and low dissolved oxygen events. Although substantially lower in nutrients compared to other Mid-Atlantic Estuaries, the biological, chemical, and ecological status of the Delaware Bay has changed in the past few decades due to high coastal tourism, increased local resident populations, and agricultural activities which have increased nutrient inputs into this shallow coastal bay. As stated by the Academy of Natural Sciences, although the nutrient load has reduced since the Clean Water Act, years of nutrient accumulation, contaminations, and sedimentation have impacted estuarine systems substantially, long-term monitoring is lacking, and ecological responses are not well quantified. Eutrophication within the Bays has degraded water quality conditions advanced by sedimentation. Understanding the quality of the water in any aquatic ecosystem is a critical first step in order to identify characteristics of that ecosystem and draw conclusions about how well adapted the system is in terms of anthropogenic activity and climate change. Determining water quality in intertidal creeks along the Chesapeake and Delaware coastlines is important because land cover is constantly changing. Many of these tidal creeks are lined with forested riparian buffers that may be intercepting nutrients from running off into the waterways. Identifying water conditions, coupled with the marsh land cover, provides a strong foundation to see if the buffer systems are providing the ecosystem services they are designed to provide. Our primary goal in this chapter is to provide research findings on the application of the hyperspectral remote sensing to monitor specific land-use activities and water quality. Along with hyperspectral remote sensing, our monitoring was coupled with the integration of remotely sensed data, global

positioning system (GPS), and geographic information system (GIS) technologies that provide a valuable tool for monitoring and assessing waterways in the Mid-Atlantic Estuaries.

Keywords: remote sensing, hyperspectral image, water quality, total suspended solids, chlorophyll-*a*, turbidity

1. Introduction

More than half of the United States population inhabits coastal and estuarine areas [1]. These regions are under pressure as rapid population growth, overutilization of natural resources, and removal of such resources as agriculture and urban development become more predominant. Although this growth and development provide economic opportunity, they also alter local ecosystems by changing land use and land cover; causing changes in soil and groundwater chemistry, watershed-level hydrology, and dissolved nutrients in waterways, particularly in the form of nitrogen and phosphorous species [2]. According to Nehrling [3], throughout the United States, commercial fertilizer use has experienced nearly a threefold increase, from approximately 6.8 million metric tons in 1960 to about 20.0 million metric tons in 2011 in order to accommodate rapid population growth and need for increased food quantities.

According to the National Oceanic and Atmospheric Administration (NOAA) National Ocean Service [4], estuaries have been seriously impacted by various anthropogenic activities and disturbances, and many are seriously degraded by pollution. Toxic substances such as chemicals and heavy metals, nutrient pollution (resulting in eutrophication), and pathogenic bacteria and viruses are the pollutants having the greatest impact on the health of estuarine waters [4]. Estuaries by their nature are transitional areas between the land and the sea including both freshwater and saltwater environments and have the accumulative impacts of both land and water activities. By far, large-scale changes from draining, filling, damming, or dredging are the greatest threats to estuaries [4]. These activities result in immediate destruction, loss of estuarine habitats, or irreversible changes in the environment.

Given the increasing number of water quality issues such as harmful algal blooms (HABs) in economically significant waters of the world, methods are needed for early detection of these issues and their sources, which when used with other environmental and historic data can alert authorities a threatening condition. Remote sensing (RS) has the potential to provide accurate synoptic views of water quality conditions over a large spatial extent and can be used to estimate turbidity and algal biomass, and have the potential to identify algal taxonomic groups. Detection of water quality issues such as dominant algal taxonomic groups can provide coastal managers with information regarding those blooms that are potentially composed of harmful algae. As such, remote sensing is an important component of overall water quality and HAB-monitoring strategy. However, coastal and estuarine waters are optically complex and the monitoring of HABs is limited in these environments by remote sensing [5].

http://dx.doi.org/10.5772/66620

Major issues facing wetland habitats include long-term changes in land cover and land use (generally including agricultural activities, habitat destruction, encroachment, and historic diking of estuarine habitat) [6], shoreline hardening, shoreline erosion, and shoreline alterations anthropogenically induced to change the structure and function of the actual marsh surface such as hydrology, marsh topography, plant community, nutrient retention, tidal flooding, detritus accumulation, and availability to secondary producers [7–11].

Land-use activities by humans cause considerable changes in the magnitude and nature of many biological, chemical, and geological (-physical) constituents that are delivered and mixed in coastal water in the Mid-Atlantic Estuaries. Consequently, monitoring intensities of changes in the estuaries and bays' water properties is important to understand the propagation and modification of terrestrial components coming from the land and also their effect on coastal environments in response to catastrophic events and climate change. However, the distributions of the biogeochemical constituents of water remain poorly understood due to limited spatial and temporal sampling. Hyperspectral remote sensing provides a continuous spectrum of radiance (or reflectance) values associated with each pixel of an acquired image to capture a unique spectral signature of water quality indicators including salinity, chlorophyll-*a* (Chl-*a*), turbidity (Secchi depth), total suspended solids (TSSs), and dissolved organic materials ((DOMs)…etc.) which act as proxies for biogeochemical exchange in various coastal waters. This type of monitoring can help to understand and quantify relationships in the spatial and temporal structure of coupled physical-biogeochemical processes for the Mid-Atlantic Estuaries ecosystems.

Remote-sensing technology can also be used as a tool to help monitor the impact of invasive species in coastal areas although this is a difficult and complex task. Ozbay et al. [12] discussed how *Phragmites australis*, the common reed, has been widespread in tidal marshes of the eastern coast of the United States in the last 50 years [13, 14] and how their abilities to supplant other wetland vegetation and decrease wetland biodiversity has attracted considerable research attention in the United States. As stated by the authors, about 10–15% of Delaware's coastal wetlands are now estimated to be invaded with tall, dense stands of *P. australis* [15, 16].

1.1. Blackbird Creek Watershed

The Delaware Bay is where the Delaware terrestrial system meets the Delaware coastal waters, leading to complex and nonlinear-mixing processes of terrestrial and marine properties. However, scientists have little knowledge of many details of the biogeochemical cycles in the bay. Furthermore, biogeochemical variability in the Delaware Bay is affected by a number of processes occurring at a wide range of temporal and spatial scales. Considering the complex and dynamic nature of the Delaware Bay water, developing a sustainable monitoring system suitable for the varying scales of the processes occurring in this region is a difficult task, especially in response to catastrophic events and climate change.

As Stone [2] stated, between 2010 and 2014, the coastal state of Delaware has grown faster than the United States as a whole—4.2–3.3%, growth, respectively [17]. The Blackbird Creek Watershed is located in southern New Castle County, Delaware, and drains roughly 80 km^2 and flows into the Delaware River just upstream from the Delaware Bay [18].

This largely semi-pristine forested watershed provides many recreational activities, and therefore varying degrees of anthropogenic effects disturb the ecosystem. Monitoring the Blackbird Creek Reserve has been on-going since mid-1970 for the detection of ecosystem changes and established management practices. Blackbird Creek is a part of the Delaware National Estuarine Research Reserve (DNERR) which is associated with the NOAA for maintaining the estuarine system. Just over a decade ago, the Delaware Department of Natural Resources and Environmental Control (DNREC) identified that roughly 36.1% of the watershed is designated for agricultural use, and an additional 13.2% for urban use [19]; **Figure 1**. However, based on more current data from the Delaware Geospatial Exchange, approximately 44% of the watershed is designated to agriculture and only about 4% to urban use.

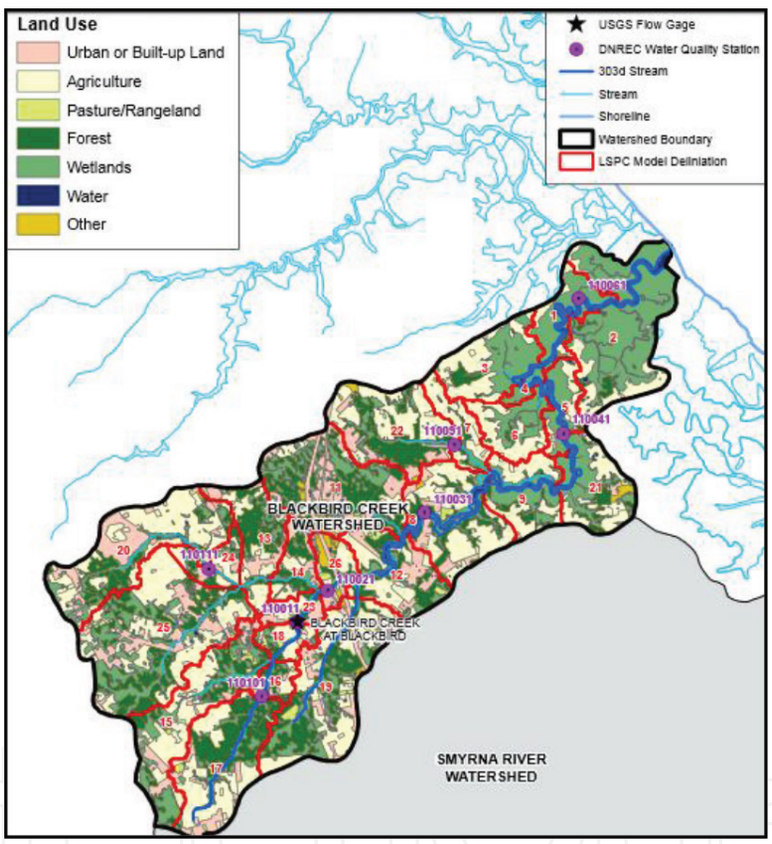

Figure 1. Land use practices in Blackbird Creek, Delaware, as described by LSPC Model Segmentation (map copied from Stone 2016, map by DNREC [19].

The Blackbird Creek tidal marsh ecosystem is dominated by various salt marsh grasses and macro fauna. Similar to many estuaries in the United States, this ecosystem is threatened by the surrounding land-use activities especially agricultural and residential activities [12].

Stone [2] reported how population growth and land-use changes put pressure on ecosystems. As the population increases, more land is cleared for development and agricultural purposes. Increased impervious surfaces from roads, parking lots, and other infrastructure can prohibit rain from entering the soil system. This can result in the conversion of the rainfall to runoff,

http://dx.doi.org/10.5772/66620

flowing into storm drains, rivers, and streams, and collecting sediments, harmful pollutants, and nutrients along the way. The monitoring of nutrient runoff into waterways and how nutrients are cycled through estuarine ecosystems are of particular importance in the Blackbird Creek Watershed. Rabalais et al. [20] and Boesch et al. [21] discussed how nutrient loading impacts streams, especially in large watersheds. Nutrients entering estuarine systems such as Blackbird Creek or the Choptank River often do so through both surface water and groundwater inputs. As Stone [2] reported, some agricultural practices, including over-tilling and unnecessary loosening of soil, over-irrigating cropland, and over-applying fertilizers, can send more soil particles and nutrients into the creek and, subsequently, into Mid-Atlantic Estuaries.

Delaware's agricultural land use has greatly impacted Delaware estuaries, in particular, poultry farming. Based on the report by the United States Department of Agriculture (USDA) cited by the News Journal [22], over 550 million broiler chickens were produced on the Delmarva Peninsula in 2012 alone, an increase of almost 14,000% since the early 1900s. According to the USDA National Agricultural Statistics Service [23], per year, Delaware state growers produced about 216 million birds alone. Poultry litter is overabundant as a by-product of the large chicken industry in the state of Delaware. Poultry litter is high in nutrients, particularly in phosphorous, and is often used as a fertilizer for pasture and hayfields throughout Delaware, including in the Blackbird Creek Watershed [24]. This litter contains high concentrations of water-soluble phosphorus and is readily transported as farm runoff. Excessive or improper fertilizer application can result in phosphorous buildup considering that the N:P ratio in plants is 8:1 while only 3:1 in poultry litter [25]. The United States Environmental Protection Agency (USEPA) identified phosphorous concentrations of 0.31 mg/L or greater to be detrimental to aquatic organisms, and is therefore the maximum value that should ever be in bioavailable form in waterways [26]. Studies have shown the detrimental impacts that phosphorous has on aquatic ecosystems, including eutrophication [27–29], mortalities of fish and invertebrates [30], and stream community shifts from a heterotrophic to an autotrophic state [31].

Major habitat change in the Blackbird Creek ecosystem is attributed to the abundance of invasive *P. australis*. Although invasive species are a less widely discussed human-caused disturbance in the watershed, it is by far the most noticeable one in the creek. Ozbay et al. [32] monitored potential impacts of *P. australis* invasion on aquatic species such as the blue crab population in Blackbird Creek Watershed to help understand the changing ecosystems in Delaware's coastal environment. Numerous studies have shown that *P. australis* invasions negatively impact essential fish habitats [33, 34]. Currently, it is not clear how invertebrates have responded to *P. australis* invasions. Research by Jivoff and Able [35] suggests that marsh surface vegetation influences the way blue crabs use marsh surface habitats. In the state of Delaware, *P. australis* is extensively studied, but most of these studies focus on the mechanism and prevention of *Phragmites*' invasion [36, 37]. Very few studies involved the detection and mapping of *P. australis* and its impact on fishery habitat in Delaware.

1.2. St. Jones River Watershed

The St. Jones River Watershed, located in central Kent County, covers 23, 327 ha (57,643 ac). This 16-km long river extends from Silver Lake Dam to the Delaware Bay. The St. Jones

Reserve, part of DNERR land, covers 1517 ha (3750 ac) and is located in the lower part of this watershed and features tidal brackish-water and salt marshes dominated by salt marsh salt hay (*Spartina patens*), cordgrass (*S. alterniflora*), and open water of creek, river, and bay areas, buffered by farmlands, freshwater-wooded fringe, and meadows but urbanized at upstream non-tidal areas [38]. It consists of three of the four hydro-geomorphic regions: poorly drained uplands, well-drained uplands, and beaches/tidal marshes/lagoons/barrier islands [39]. In the St. Jones Watershed, 39% of wetlands are tidal salt or brackish marshes, 35% are freshwater flats and 24% are riverine wetlands, and less than 2% are freshwater tidal or depressions [40]. There are several unique and threatened wetland features including bald cypress, Atlantic white cedar, and coastal plain ponds [40].

Agriculture and developed land in the St. Jones Watershed comprise almost 70% of the entire watershed's acreage. **Figure 2** shows the distribution of land use across the watershed from the National Land Cover Dataset (NLCD). Agricultural land and non-tidal wetlands are spread throughout the watershed. While forested patches are mainly located in the northern portion, large areas of tidal wetlands occur in the southeastern portion of the watershed. Since 2002, this watershed has experienced significant changes in land use and cover. The conversion of farmed land into residential housing led to a 6.1% increase in developed land and a 6.5% decrease in agricultural land. There were also losses in freshwater wetlands, particularly in non-tidal forested and scrub-shrub wetland habitats [41].

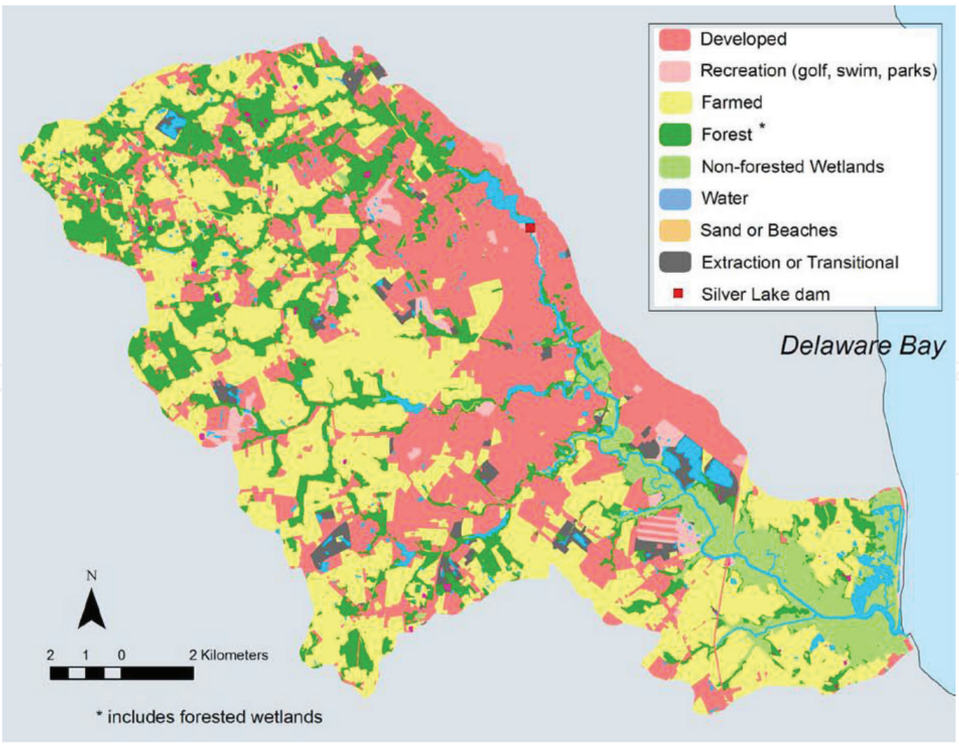

Figure 2. Land cover for the St. Jones River Watershed in 2007 based on National Land Cover Dataset (NLCD) land use categories [42].

http://dx.doi.org/10.5772/66620

Water quality problems in the St. Jones Watershed are attributed to sediment, nutrient, and chemical runoff [39]. Non-point pollution sources including runoff are mainly from roads (potentially containing oil, antifreeze, salt, and/or gas), lawn fertilizers and pesticides, and so on, dominate the St. Jones Watershed. Wastewater from septic systems is a source of nutrients in groundwater [39]. Moreover, channelization and ditching for agriculture and mosquito control led to altered natural wetland functions [39]. In addition, the invasive species such as *P. australis* have spread throughout fresh to brackish wetlands [39].

Rogerson et al. [42] reported that tidal sites with higher wetland condition scores resulted in lower avian species richness composed of primarily wetland-specific species, based on the intensive surveys of the avian community and vegetative biomass. Unfortunately, large areas of headwater flats in St. Jones River Watershed have been lost due to mainly agricultural production and development. According to Rogerson et al. [42] "Thirty-five percent of wetlands across the watershed were flats and had an average condition of 81, ranging from 57 to 94. Using condition categories, 37% of flat wetlands were minimally stressed, 47% were moderately stressed, and 16% were severely stressed." Over the last 50 years, over half (53%) of the 1385 ha of flats had not been forested (e.g., clear-cut, selective cut). As stated by Rogerson et al. [42], "Flats in higher condition had minimal garbage or dumping, low coverage by invasive plants, minimally altered micro-topography, and had a low occurrence of wetland ditching." Based on their assessment, forestry activity including cutting and harvesting within wetlands, and development and agriculture in buffers seem to be the major source of stressors in the watershed. Per Rogerson et al. [42], "Riverine wetlands, found adjacent to streams and rivers, accounted for 24% of the watershed's wetland acreage and had an average condition score of 72. Over half (55%) were considered minimally stressed, with low occurrences of invasive species, fill, and ditching, but frequently had dumping in addition to development and roads in the buffer. The severely stressed portion (10%) had condition scores as low as 27, related to the high prevalence of forestry activity, dumping, fill, storm water inputs and development within the buffer." They noted that wetlands with greater condition scores result in greater amounts of total-below ground biomass and a greater ratio of total-above-to-total-below ground biomass. Developmental activities such as residential, commercial, and/or transportation in the 100-m assessment site buffer were strongly related to the occurrence and frequency of wetland stressors such as storm water inputs, garbage, dumping, and invasive plants.

The watershed wetland condition report by Rogerson et al. [42] provided site-specific recommendations to improve wetland management, maximize natural benefits of tidal and non-tidal wetlands, and encourage informed decisions concerning the future of wetlands in Delaware. Previous research by Tiner [41] confirmed that the Delaware Bay basin was converted significantly to agriculture and residential development, particularly in non-tidal forested and scrub-shrub wetland habitats in St. Jones River Watershed. Emergent tidal wetland losses resulted in the excavation and filling of hydric sediments and the creation of impoundments [41]. As stated by Rogerson et al. [42], changes in land-cover and land-use patterns, especially near wetlands, are important to consider when evaluating wetland condition and its health.

1.3. Chesapeake Bay Watershed

The Chesapeake Bay—the largest estuary in the United States—is an incredibly complex ecosystem that includes important habitats and food webs. The Chesapeake Bay watershed spans more than 16,575,900 ha and encompasses parts of six states—Delaware, Maryland, New York, Pennsylvania, Virginia, and West Virginia—and the entire District of Columbia. Almost 18 million people live in the Chesapeake Bay watershed. The Chesapeake Bay's land-to-water ratio is 14:1: the largest of any coastal water body in the world. It is a very productive ecosystem that supports important recreational and commercial fisheries [43]. As shown in **Figure 3**, anthropogenic activities on land have a large impact on the Bay's health, most importantly; the water quality in Chesapeake Bay has declined significantly in recent decades, driven by the human population growth and changes in land use that together increased the nutrient loads [44].

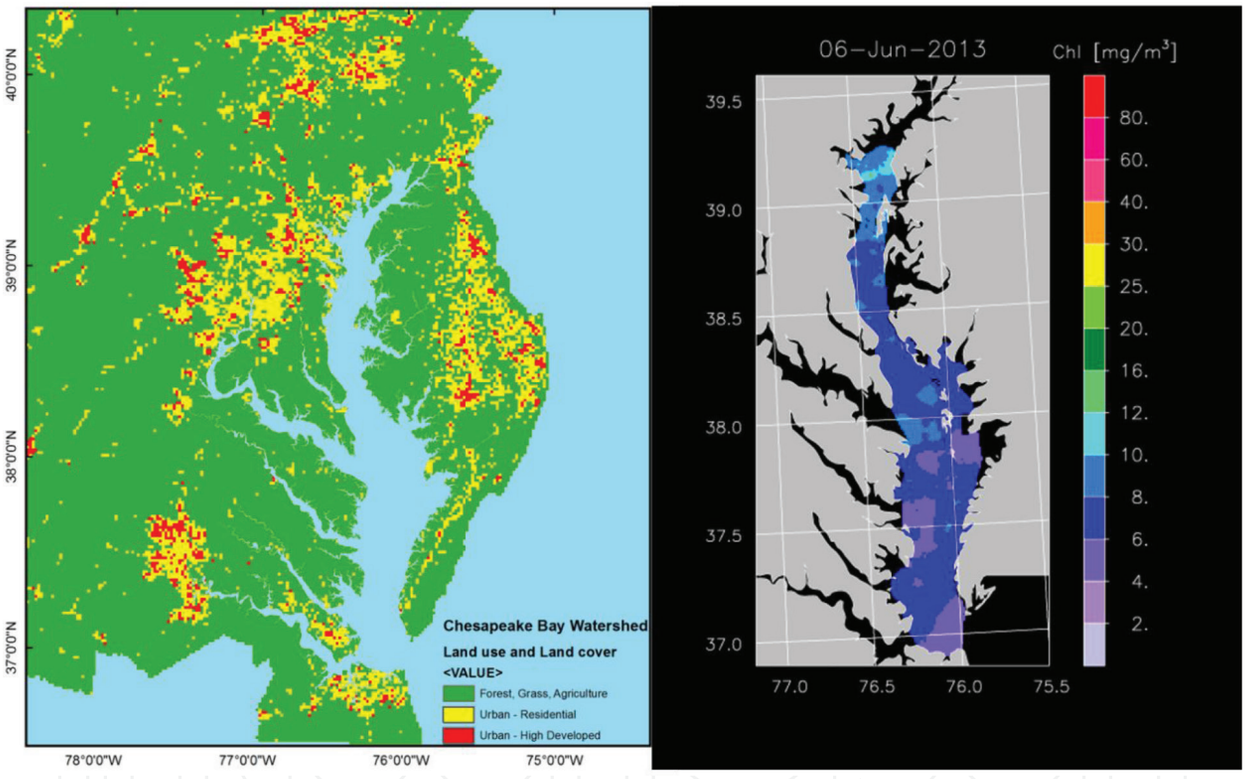

Figure 3. Chesapeake Bay Watershed land use and land-cover map showing majority land uses for forest, grass and agricultural activities and residential development (data from MD DRN LULC 2010 census), and the surface Chlorophyll-*a* concentration in the Chesapeake Bay by aircraft remote sensing in 2013 [45].

Soil and water quality protection are major challenges that must be addressed in modern day agricultural systems. Fifty billion liters of water flow into the Chesapeake Bay from over 150 streams and rivers. It supports more than 2700 species of plants and animals and produces 227 million kg of seafood each year. However, today, various factors have negatively impacted water quality and the deterioration of the overall health of the bay ecosystem. The Chesapeake basin water is highly impacted by agricultural development, residential development, effluent discharge from sewage treatment plants, and residential development

http://dx.doi.org/10.5772/66620

by Pennsylvania Association of Conservation Districts, Inc. [46]. Point and non-point source (NPS) pollutants have caused ecosystem eutrophication which stimulates hypoxia, anoxia, frequent fish kills, increased turbidity, loss of submerged aquatic vegetation, and changes in food web structure [21]. Excess nutrients and sediment pollution originated by the agricultural activities in Delmarva's tributaries are a major concern.

According to Chesapeake Bay Foundation Report [47], the three major contributors to the poor health of the Chesapeake Bay include nitrogen, phosphorus, and sediment. As stated in the report, excess nitrogen and phosphorus fuel unnaturally high levels of algae growth in the water, blocking sunlight from reaching submerged aquatic vegetation such as grass bed that serve as food and habitat. In addition to hindering the growth of aquatic vegetation, algal die-off results in an increase in bacterial population that decomposes the dead algae and aquatic vegetation, as well as consumption of dissolved oxygen in the water. The Chesapeake Bay Foundation Report [47] states that fertilizers, wastewater, septic tank discharges, air pollution, and runoff from farms, cities, and suburbs result in excessive nutrients.

Erosion, coastal alteration, and construction-related development result in excessive amounts of sediment. Excessive sedimentation from tiny particles of dirt, sand, and clay floating in the water clouds the water, blocking sunlight from reaching submerged aquatic vegetation. Aquatic species such as oysters, a keystone species, and other bottom-dwelling organisms can be smothered when that sediment finally settles to the bottom. Major sources of pollution in the Chesapeake Bay include agricultural runoff by 41%, air pollution by 25%, wastewater treatment and factories by 16%, urban and suburban storm water runoff by 15%, and septic tank failures and leaks by 3%. As the major contributor to the pollution, agricultural runoff includes animal waste and fertilizers which wash off agricultural land or contaminate groundwater, which in turn pollute rivers and streams, and the Bay. **Figure 4** illustrates these pollutants and their origins [47].

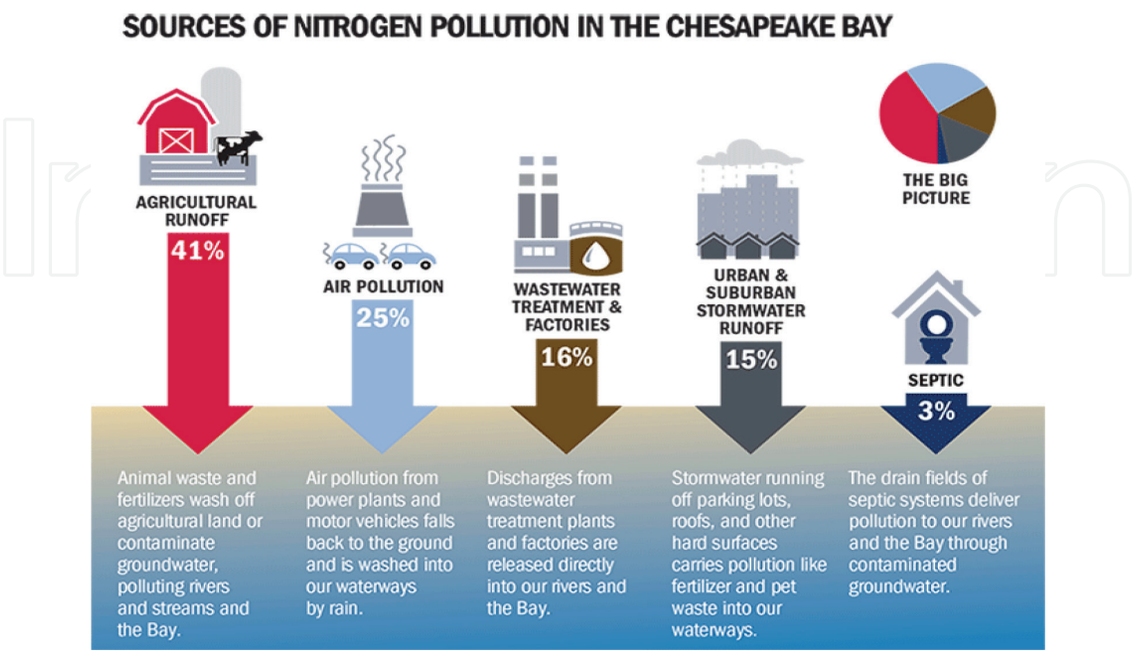

Figure 4. Illustration shows the sources of nitrogen pollution in the Chesapeake Bay [47].

Specifically, the waste from poultry production has raised serious concerns about treatment and disposal of the chicken manure along the shores of the Chesapeake Bay. With over 12 million cubic meters of chicken waste produced by over 523 million chickens produced each year in just Maryland and Delaware alone, serious risks in the coastal states have been raised. Diminishing crop lands have led to an increased use in manure load limits for cropland soil enrichment, resulting in excess nutrients from the poultry farms to flow into the ditches, streams, and rivers feeding into the Chesapeake Bay [48]. According to Ogejo [49], regardless of the size or type of farm, animal, livestock, and poultry producers need to manage manure for better economic returns and environmental protection. Similar to other basins in the mid-Atlantic, the Chesapeake water basin is excessively impacted by agricultural development, residential development, habitat loss, and effluent discharge from sewage treatment plants [50].

1.4. Remote sensing: multispectral and hyperspectral analyses

During the last few decades, remote sensing has allowed continuous monitoring opportunities of areas and objects over longer period and larger scale on Earth [51]. According to NOAA [52], remote sensing basically is the science of obtaining information about the areas or objects from a distance such as a satellite or an aircraft. As they stated, remote sensors, which can be on satellites or mounted on aircraft, collect data by detecting the energy that is reflected from Earth. Those sensors are either passive or active sensors. The most common source of radiation detected by passive sensors is reflected sunlight, while active sensors such as a laser-beam remote-sensing system use internal stimuli to collect data about Earth [52]. **Figure 5** shows an example of the Chesapeake Bay: Land Remote Sensing Image by using A Landsat 8 Surface Reflectance Mosaic by United States Geological Survey [53].

Figure 5. Chesapeake Bay land remote-sensing image by using A Landsat 8 Surface Reflectance Mosaic on April 4, 2016 [53].

http://dx.doi.org/10.5772/66620

Coastal waters are under increasing pressures from anthropogenic disturbances at various temporal and spatial scales [54, 55]. Water quality monitoring is vital for assessing such impacts, and further provides important information for sustainable water resource managements. Water quality analysis is an extremely important tool used to determine the overall health of an aquatic ecosystem, as a healthy environment will impact aquatic life forms and affect how they interact with the environment and each other. We are identifying how land use affects water quality, especially as it pertains to direct human interaction and indirect runoff from agricultural fields. Estuaries receive continuous inputs of biogeochemical constituents from their fresh water sources. For example, discharge of nutrient-rich water from urban, forest, salt marshes, agriculture, and ranching areas increases organic and inorganic sediments accumulation in Blackbird Creek. Nutrients can be measured by monitoring water quality and estimating distributions of matters in water bodies [56]. Although a wealth of new knowledge generated over the last several decades about these ecosystems, the spatial and temporal patterns of biologic and physical processes as well as anthropogenic influences are not fully understood.

While traditional monitoring programs can provide valuable water quality information, these programs are time and labor intensive, and lack the necessary temporal or spatial information needed for better decision making. Remote sensing offers the most effective means for frequent, synoptic water quality measurements [57–59]. Remote sensing offers a unique perspective because of the synoptic view and those quantitative algorithms can be used to extract geophysical and biophysical information [60]. Optically complex estuarine environment such as Blackbird Creek can be accurately mapped, measured, and characterized using remote-sensing techniques in order to develop models to map water quality characteristics of estuaries and freshwater tidal wetlands.

Ozbay et al. [12] discussed how recording the presence of *P. australis* within a tidal marsh zone presents challenges in the physical execution of a vegetation survey in an environment with restricted mobility, an overall study region with an area measurement on the order of tens to hundreds or even thousands of square kilometers, as well as the accuracy of species identification via sensor capabilities and various classification methodologies. Remote sensing utilizing satellite or aerial imagery enables one to more to easily collect data from afar without having to be physically present in harsh environments. Likewise, remotely sensed imagery can be collected at various resolutions, providing detail on a multitude of scales. Lastly, various algorithms and sensor capabilities provide varying degrees of accuracy for species identification.

According to GIS Geography [61], multispectral and hyperspectral remote sensing are being used for many applications in the fields of agriculture, ecology, oil and gas, oceanography, and atmospheric studies to better understand the world we live in [61]. However, their applications are depending on the information needed. Having a finer spectral detail in hyperspectral images gives better capability to see the unseen in finer details such as specific fish population in water. Technically, the main difference between multispectral and hyperspectral is the number of bands and how narrow the bands are to one another. Per GIS Geography [61] "multispectral imagery generally refers to 3 to 10 bands that are represented in pixels.

Each band is acquired using a remote sensing radiometer. Hyperspectral imagery consists of much narrower bands (10-20 nm). A hyperspectral image could have hundreds of thousands of bands. This uses an imaging spectrometer." According to Fisher et al. [62], "a collection of several monochrome images of the same scene taken by a different sensor makes a multispectral image that we referred them as a band. Multi-band image also called as multi spectral is a RGB color image that consists of a red, a green and a blue image taken with a sensor sensitive to a different wavelength". Example is provided as hyperspectral remote sensing distinguishes between three minerals because of its high spectral resolution while the multispectral Landsat Thematics Mapper could not.

An example given by Ozbay et al. [12] provided a comparison of the application of multispectral versus hyperspectral imaging with an important factor in the classification or monitoring of a wetland species, such as *P. australis*, where utilizing remotely sensed data involved the concept of scale. The extent of an intended study area has a great impact on the necessary available data to analyze. As discussed by Ozbay et al. [12], a sensor with high spatial resolution provides finer detail compared to a medium-resolution sensor over the same geographic area. If a specific area has a large geographic extent, the use of satellite imagery with a coarse resolution (10–30 m), such as *Landsat* Thematic Mapper (TM) or Le Systeme Pour l'Observation de la Terre (SPOT), may be sufficient. However, if the primary interest is on the order of several hundred meters or a few kilometers in lineal extent, aerial photography or the use of high-resolution (1–4-m) imagery, such as IKONOS or *QuickBird*, may be more appropriate or beneficial. The use of imagery with high spatial resolution may not necessarily result in improved detection or classification accuracy.

In general, multispectral data can be useful to determine broad vegetation classes and hyperspectral data can be effective to differentiate vegetation classes at the species level [12]. Authors noted that high-resolution imagery or hyperspectral data can lose effectiveness because of different vegetation species with similar biochemical and biophysical properties [63]. They also discussed that results may suffer due to spectral variations in the same species as a result of age differences, soil and water background, or stresses most notably in the near- to mid-infrared bands issues.

Classification of various wetland vegetation species including *P. australis* poses a complex challenge utilizing remote-sensing techniques. As stated by Shippert [64], standard multispectral image classification techniques are generally developed to classify multispectral images into broad categories while hyperspectral imagery provides an opportunity for more detailed image analysis for specific narrow range. Hyperspectral data-derived vegetation classifications generally are possible due to the ability to distinguish species using known reference spectra or spectral libraries.

As stated by Ozbay et al. [12], the cost of field validation of multi- or hyperspectral imagery is relatively high, limiting the use of remote-sensing data due to the uncertainty of the classifications required to manage natural resources [65]. A small wetland site may be adequately and reasonably covered with high-resolution satellite imaging. On the other hand, if the size of a study site becomes larger, it will become more cost-effective to utilize medium-resolution

http://dx.doi.org/10.5772/66620

satellite imagery over high-resolution satellite imagery. As stated by the authors "Whereas aerial photography may be suitable for smaller wetlands or non-frequent observations, mapping or monitoring on a regional scale and increased frequency with such imagery would be costly and time-consuming to process."

Hyperspectral remote sensing provides a new class of Earth observation data for improved Earth surface characterization. For example, it has been used accurately to characterize complex coastal environments [66, 67] and has the potential for mapping and detecting harmful algal blooms [68], major sediment pigments of benthic substrates [69], and suspended particulate matter [70]. The high spectral resolution provides the opportunity to develop and evaluate advanced methods of spectral shape analysis, such as derivative spectroscopy that can accurately distinguish subtle features in spectra and may be critical for discriminating optically significant water constituents [71, 72].

Various empirical, semi-analytical, and analytical ocean color models have been developed last few decades to derive the water quality parameters of interest such as concentrations of total suspended solids (TSS), chlorophyll-*a* (Chl-*a*), and the absorption of colored dissolved organic matter (CDOM)) [73]. However, coastal and estuarine waters are optically complex and the signal that a remote-sensing detector collects is a mixed signal composed of various water optically active constituents from different sources [59]. For the case of the mixing of two waters, attempts to apply the ocean color models could result in poor predictive ability in retrieval of various water quality proprieties [74].

Jo et al. (unpublished data) [75] discussed the advantage of using high spectral and spatial resolutions as they illustrated in **Figure 6** where **Figure 6A** shows chlorophyll-*a* concentration in the Delaware Bay, calculated from MODIS data (500-m spatial resolutions), **Figure 6B** shows the Enhanced Thematic Mapper Plus (ETM+) (30-m spatial resolutions) on the same day, and **Figure 6C** shows an aerial photograph from the Helikite (Helium Kite, http://www.allsopp.co.uk/) at around 30-cm spatial resolution to monitor specific locations such as oyster beds continuously [76].

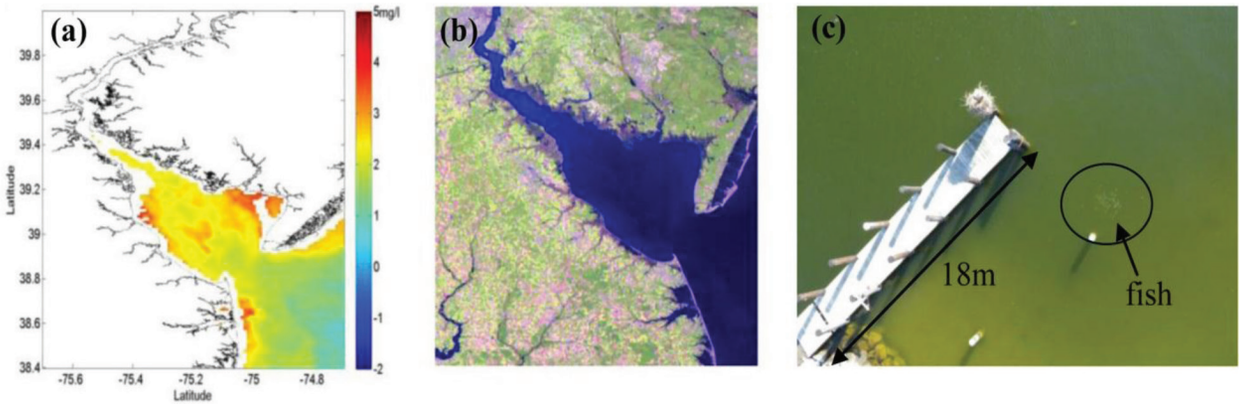

Figure 6. (A) Chlorophyll-a concentration from MODIS at 500-m spatial resolution; (B) combined three bands from ETM+ of Landsat 7 at 30-m spatial resolution; and (C) aerial photo of Helikite at 30-cm spatial resolution in August 31, 2011 (Jo et al. unpublished data) [75].

1.5. Water quality: suspended solids, turbidity, phosphorus, and chlorophyll-*a*

The water quality conditions in many fresh and coastal marine systems have progressively declined as the human population increases last century. This is often in response to increased runoff of nutrients from encroaching agricultural and urban areas due to housing development [77–79].

Over half of the Blackbird Creek Watershed is composed of agricultural lands. These lands are fertilized heavily to accommodate the timely growth of corn, soybeans, and sorghum grass. This fertilization is a concern for marsh habitat and local nekton of commercial and ecological importance. The excess nutrient loading tends to favor the growth of aggressive, invasive, often weedy, plant species which displace native plants. In extreme cases, nitrogen and phosphorous loading cause algae growth so great that the blooms block out sunlight to submerged aquatic vegetation, a crucial habitat for larval and juvenile fish and crabs [78, 79].

Stone [2] discussed that the overabundance of both reactive nutrients and non-reactive constituents can be detrimental to the quality of waterways, while they may not be acutely toxic. Turbidity is a measure of how clear or cloudy a water sample is and, by proxy, a suitable measurement to determine suspended sediments and solids which could settle out onto the riverbeds and banks [80]. Davies-Colley and Smith [81] reported that sediments in suspension can have the potential to smother benthic biota, irritate fish, crab and shellfish gills, and transport adsorbed contaminants. While sediments do have the capability of settling out, there is also a potential for them to remain in suspension and reduce the visual range of sighted organisms to seek out prey and/or members of the opposite gender for reproductive activity. High turbidity reduces the light penetration into the water and lowers the amount of available light availability. This, in turn, reduces the amount of phytoplankton production, possibly impacting higher trophic levels in a bottom-up model [82–85].

De Robertis et al. [83] and Kirk [86] documented the role of phosphorous in receiving waters. In systems like Blackbird Creek and Choptank River, the contribution of phosphorous to surface water is more likely from crop fields instead of household wastewater. Olli et al. [87] discussed that most of the phosphorous is generally in the form of bound reactive phosphate attached to eroded particles that have run off into the surface water not readily available for uptake by plant. On the other hand, Correll [88] and Reddy et al. [89] reported that phosphorous was retained in water and sediments via adsorption, complex formation, chemical precipitation, and biogeochemical reactions or recycled in the system. The compounds may be enzymatically hydrolyzed to form orthophosphate once phosphorous enters the water. This is the only form of phosphorus that can be taken up by algae, plants, and bacteria.

Blackbird Creek and other Mid-Atlantic watersheds influenced by agricultural land-use practices are susceptible to phosphorous enrichment. Many agricultural crops that are grown adjacent to waterways are treated with fertilizer containing high phosphate concentrations. As most of the phosphorus that enter aquatic environment precipitate by interacting with cations, phosphorous in freshwater can be retained in sediments by interactions with cations

such as iron (Fe) and aluminum (Al). In seawater environments, deposited phosphorous is in large part returned to the overlying water through remineralization, making it biologically available for the consumption of phytoplankton and have better cycling of phosphorus [90].

RMB Environmental Laboratories Inc. [91] reported that chlorophyll-*a* is a green pigment in plants, algae, and phytoplankton that allows photosynthesis. The amount of phytoplankton growth in water bodies depends on various factors such as water temperature, water transparency, predation by zooplankton, and the availability of phosphorus and nitrogen (nutrients). Natural seasonal variations changed phytoplankton concentrations, and drastic changes in the abovementioned parameters due to hurricanes, storms, heat waves, and so on have detrimental effects on overall phytoplankton diversity and biomass [92]. Per RMB Environmental Laboratories Inc. [91], spring time, water is more transparent while there are more nutrients available due to the spring turnover; however, the water temperature is still low and this limits algal growth. As the water temperature increases during the summer, algae grow and its concentrations are higher. More nutrients can get washed into the lake if there are heavy rains that trigger more algal blooms. With increase in algal concentration, water becomes less transparent. Ritchie and Cooper [93] reported that eutrophication can be quantified by the concentration of chlorophylls contained in phytoplankton. According to USEPA (2000), monitoring the concentration of chlorophylls in phytoplankton can be used to evaluate and control eutrophication in water bodies.

According to Fondriest Environmental Inc. [94], the concentration of chlorophyll-*a*, as the green pigment used by phytoplankton in photosynthesis, is a good indicator of the amount of phytoplankton biomass in aquatic environments. Chlorophyll-*a* concentrations can be monitored in several forms consisting of chlorophylls a, b, c, d, and e. Concentrations of those forms determine the trophic state of water bodies, and high concentration most often indicates eutrophication [94].

Chlorophyll-*a* concentration estimated from the blue-to-green ratio of water-leaving radiances is used as a proxy for the phytoplankton biomass—for its distribution, variability, and growth rate studies [95]. This approach has been very successful in providing data for global distributions of algal biomass and in formulating estimates of global ocean primary production [96]. Nevertheless, knowledge of chlorophyll-*a* concentration is not sufficient to properly assess the biogeochemical and geophysical properties of the ocean surface layer [97].

Stumpf et al. [98] published results on monitoring *Karenia brevis* blooms in the Gulf of Mexico using SeaWiFS ocean color imagery, and indicated "the need to detect *Karenia brevis* blooms requires additional capability than simply identifying chlorophyll patterns." The capability of determining algal taxonomic composition can yield important information about overall water quality, eutrophication, and the distribution of HABs. A shift in algal species composition can be an important indicator of changes in water quality and may have serious environmental repercussions [99]. Therefore, the capability of determining this composition, as well as an estimation of algal biomass (chlorophyll-*a* concentration), by remote sensing is needed for the detection and monitoring of HABs. These data, when combined with other data, such as in situ data of nutrients and meteorological data, can potentially create models to forecast the development of blooms and HABs.

Stone [2] reported "as climate changes, it is simply not possible to discuss aquatic ecosystems without a detailed description of current and future trends in temperature, salinity, dissolved oxygen, pH, and the interactive effects of each of these variables on each other. This is also true with respect to change in land use. When land is modified to accommodate human needs, surface runoff, evapotranspiration, stream discharge, and sediment transport are all influenced, which in turn could have implications on the aforementioned parameters. If there is greater runoff from a crop field that was converted from a forested wetland, for example, there may be increased turbidity, reduced water temperature, and lower salinity. The potential ramifications in such a scenario would be monumental." The integrated use of remotely sensed data, geographic information system (GIS), and global positioning system (GPS) has enabled natural resource managers, state and federal governments, and consultants to develop management plans and policies for a variety of natural resource management applications for long-term sustainable options [100].

2. Case studies

Following case studies provide research-based discussion on the application of hyperspectral remote sensing and its specific modification for the research needs. In this chapter section, our primary focus is on Mid-Atlantic Estuaries, specifically Blackbird Creek Watershed, St. Jones River Watershed, and Chesapeake Bay Watershed.

2.1. Geographic information system (GIS) and remote sensing (RS) application in land-use classification and its relationship with water quality

Blackbird Creek is characterized by extensive salt marshes and large native populations of the salt marsh cordgrass (*S. alterniflora*). Blue crabs, as well as several other ecologically and economically important aquatic species, prosper in salt marsh environments where the leaves, roots, and stems of native plants provide sources of food and shelter from predators for many juvenile animals. Much of Delaware's other coastal wetlands including Blackbird Creek has been subject to a loss of biodiversity over the past several decades due largely to the common reed (*P. australis*) invasion. As reported by Roeske [101], this may be considered a highly disturbed ecosystem due to the invasion of *P. australis* and the intensive management (i.e., herbicide spraying) that have occurred since the early 1990s. Roeske [101] also reported that glyphosate is one of the most widely used herbicides in the world, especially with the advent of genetically modified organisms (GMOs), giving outcome to glyphosate-resistant crops. This chemical is referred to as a systemic, broad-spectrum herbicide, killing plants only a few days after application by blocking an enzyme that is vital in the production of amino acids and proteins [102]. Sadly, glyphosate is not species specific and generally kills all marsh vegetation. Roeske [101] stated that the long term and most effective management strategies for the control of *P. australis* have utilized a combination of the removal techniques including mowing, burning, herbicide treatment, increased salinity, and so on. These conditions encourage native plant colonization while pushing out non-native *Phragmites* by providing constant stress through these removal techniques. Roeske [101] also discussed that burning alone may actually reinvigorate the populations in subsequent years and thus these methods must be utilized in a strategic manner over the course of several growing seasons if any permanent removal is to be accomplished [103].

http://dx.doi.org/10.5772/66620

Stone [2] reported that ecologically and economically important resident fish and crustacean species in Blackbird Creek can be impacted indirectly by phosphate loading. Increased nutrient concentrations can increase phytoplankton productivity in aquatic ecosystems, which in turn can result in a drawdown of oxygen via increased respiration and decomposition of algae. Lowery and Tate [104] reported that dissolved oxygen reductions to less than 2 mg/L resulted in an increase of blue crab hemolymph lactate activity.

High sediment concentrations in tidal creeks and estuaries are possibly due to transport through the catchment basin via tidal activity and wind-induced sediment resuspension [105], especially when land is modified to accommodate human uses. Wischmeier and Smith [106] reported a strong chance of the erosion of sediment from recently tilled land on any kind of slope due to rain and wind, and subsequent runoff into waterways, which could lead to a variability in light availability on the scale of hours (tides) and days (calm vs. windy days). In systems such as Blackbird Creek, primary production may be compromised due to diminished light penetration which could result in reduced zooplankton production and lead to lower recruitment of estuarine species [107], thus altering the flow of energy through food webs since the autotrophic base would not be efficient enough to sustain higher trophic levels [108].

Agricultural land use in the Blackbird Creek Watershed was identified using ArcGIS layers available in the Delaware Geospatial Exchange. To select agriculture treatments, the watershed was gridded out into 500 × 500-m cells and the percentage of agricultural land cover within each cell was calculated. Water quality analysis was conducted based on these treatments in the Blackbird Creek. Any correlation between orthophosphate concentration and turbidity in relation to the land use based on the percent agricultural use was the main focus of the project (**Figure 7**).

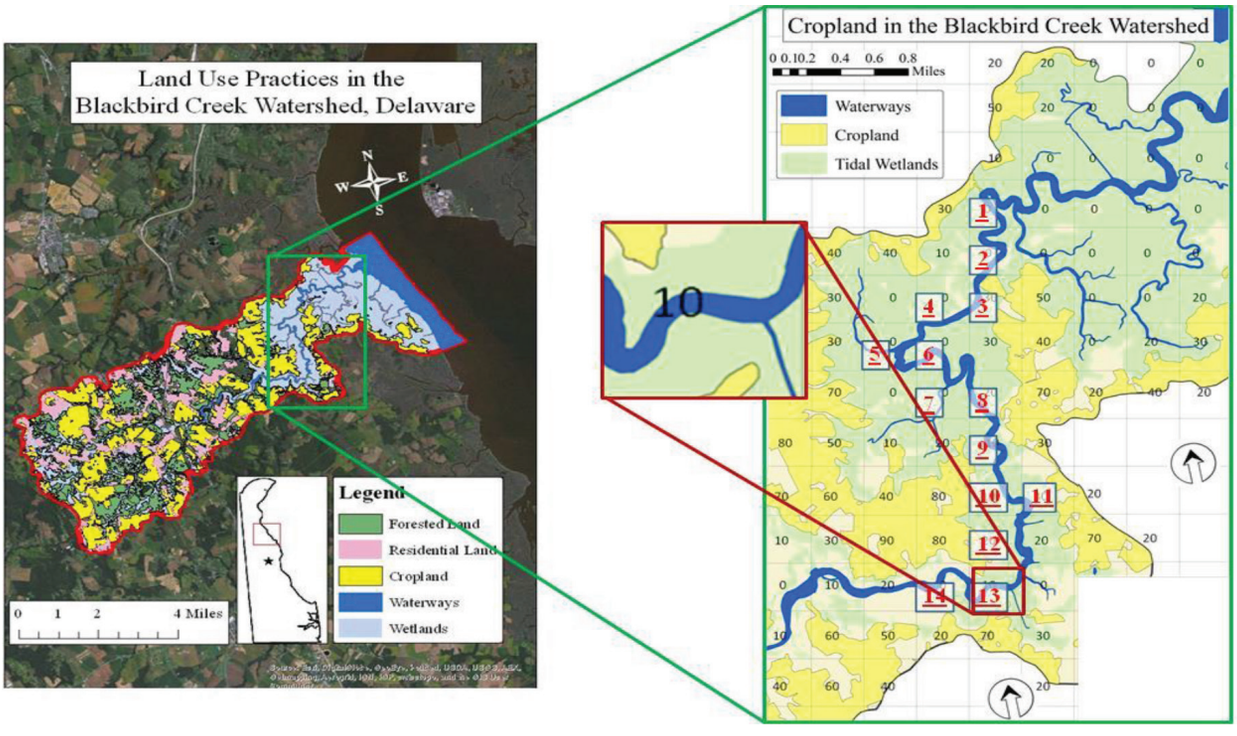

Figure 7. Sampling strategy shows the grid navigable tidal watershed into 500 m × 500 m cells and identifies the percentage of agriculture land cover in each cell. Samples were taken within each cell and differences of dependent variables across the percentages of agriculture were tested [2].

A considerable body of literature is available that explains the role of non-point source phosphorous runoff plays in the eutrophication of receiving water [109]. For agricultural watersheds such as Blackbird Creek, fertilization of soils greater than the total crop phosphorus uptake requirements leads to a buildup of phosphorous in the soil over time [110]. Studies have shown the positive relationship between soil phosphorus and surface water phosphorus, especially during high discharge events [111], indicating an association between soil management practices and surface water phosphorus concentration.

Holliday et al. [112] found 1:1 correlation between turbidity and total suspended solids for silt and clay fractions, but a smaller ratio for bulk-soil samples. Nevertheless, their research suggested that turbidity can be used to estimate sediment concentrations for fine soil fractions, which is, what the mouth of Blackbird Creek is primarily composed of. Other research has shown that reactive phosphorus increases with increased total suspended sediment concentrations [87–89, 113]. Based on these studies, our first goal was to identify trends in orthophosphate in accordance with measurements of turbidity.

Collection of water samples was undertaken over the course of 4 years (2012–2015) at various times of day between March and November. At each site (**Figure 7**), water was collected into dark polyethylene bottles (rinsed three times with sample water), then placed on ice for transport to the laboratory for nutrient analysis where samples were measured for orthophosphate and turbidity concentrations. Because orthophosphate is reactive in nature, a subsample of water was filtered on site into a separate bottle in order to minimize the potential for such reactions. Orthophosphate concentrations were determined using HACH Method No. 8048, the ascorbic acid method. This reaction provided information on soluble reactive phosphate concentrations between 0.02 mg L^{-1} PO_4^{3-} and 2.50 mg L^{-1} PO_4^{3-}. The measurements were performed using a HACH DR 3900 spectrophotometer (HACH, Loveland, CO). Turbidity was measured with an automatic wavelength selection on a YSI 9500 Photometer (YSI Incorporated, Yellow Springs, OH) and presented in Formazin Turbidity Units (FTUs), which is generally equivalent to Nephelometric Turbidity Units and Jackson Turbidity Units (JTUs). This method allowed for measurements between 5 and 400 FTU.

Based on the data by Stone [2], there were no correlations between turbidity and orthophosphate concentration. Linear regression analysis showed that there was a negative trend between the two parameters ($y = -5.0822x + 52.734$), but with an r^2-value of 0.0016, this cannot be considered statistically significant (**Figure 8**). It did appear that the tidal regime was important with respect to the turbidity concentration. On incoming tides, there was a negative trend ($y = -20.486x + 52.776$; $r^2 = 0.0628$) (**Figure 9**), whereas on outgoing tides, there was a positive trend ($y = 20.619x + 46.201$; $r^2 = 0.0175$) (**Figure 10**). Neither of these trends was significant, but it is interesting to note the opposite slopes as they relate to the tidal movement upon collection. When the tide was receding, there was a positive slope in the data. Thus, orthophosphate concentration was greater with greater turbidity, while the opposite was true on incoming tides. It is hypothesized here that this could be due to the source of these parameters as they regard the tide. On incoming tides, there was greater phosphorus concentration (0.62 mg PO_4^{3-}/L ± 0.020 SE) than on outgoing tides (0.55 mg PO_4^{3-}/L ± 0.024 SE). On incoming

http://dx.doi.org/10.5772/66620

tides, there was less turbidity (38.72 FTU ± 1.776 SE) than on outgoing tides (47.72 FTU ± 2.965 SE). Other unpublished research [101] has shown that orthophosphate concentrations upstream were considerably lower than those that were found at the sites from this study. Thus, it may be suggested that the positive trend line in the data on outgoing tides could be a function of reduced orthophosphate at the source and/or the size fractions of the sediment particles in the upstream portion of the tidal creek. Further research is necessary to verify this postulate.

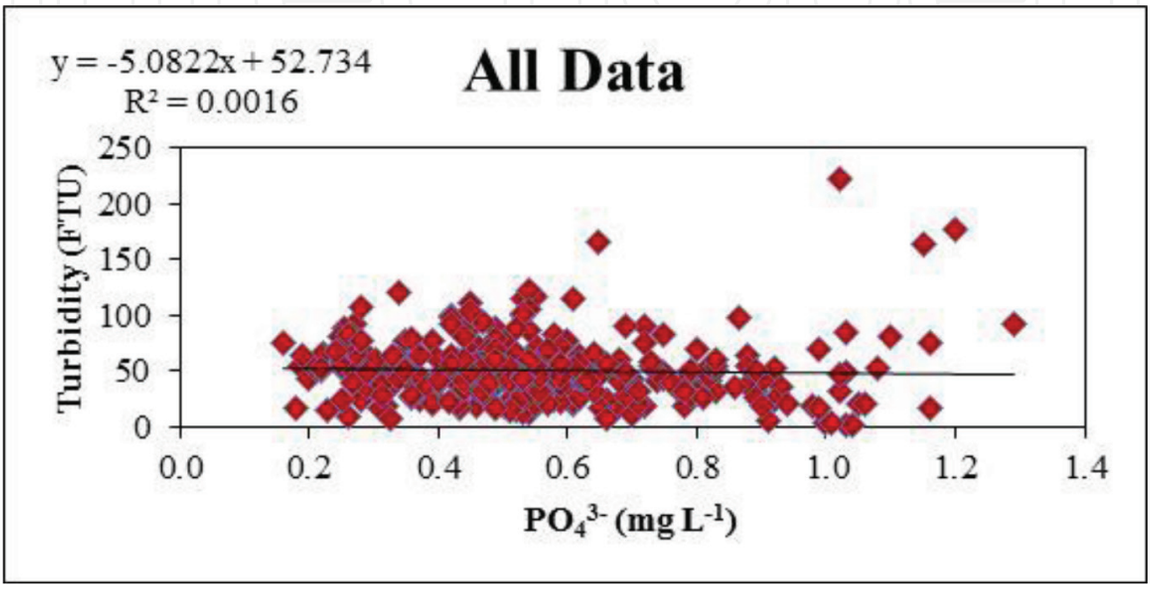

Figure 8. Correlations between turbidity and orthophosphate (PO_4^{3-}) concentration for both incoming and outgoing tides water [2].

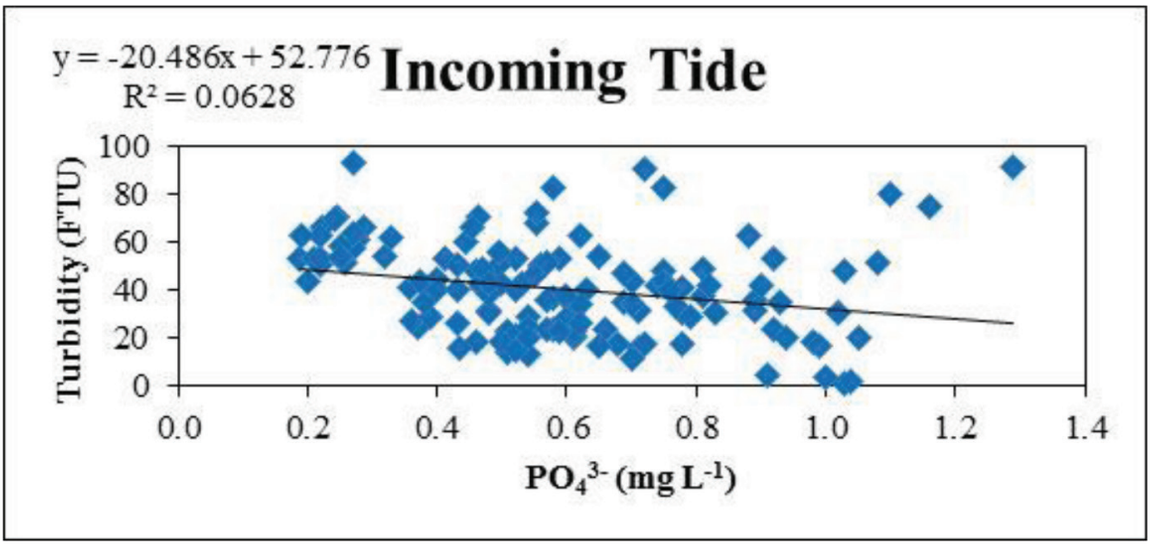

Figure 9. Correlations between turbidity and orthophosphate (PO_4^{3-}) concentration for incoming tide water [2].

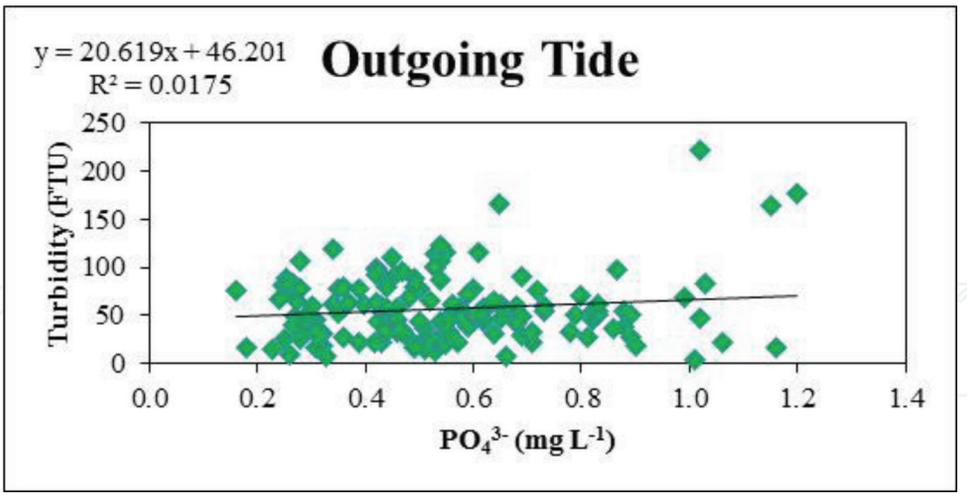

Figure 10. Correlations between turbidity and orthophosphate (PO_4^{3-}) concentration for outgoing tide water [2].

2.2. Application of AISA hyperspectral analysis in investigation of total suspended solids and chlorophyll-*a* in the Blackbird Creek, Delaware

The many biogeochemical processes taking places in estuarine environments maintain ecosystem health. Estuaries have a resilience to change, as long as the disturbance has not reached the threshold of where changes can no longer be reversed. A report by the Department of Interior, in conjunction with the U.S. Fish and Wildlife Service Dahl [114], states that over the past two centuries the continental United States has seen a 53% reduction in total wetland acreage, with Delaware losing approximately 54% of its original wetland habitat. It is generally accepted that this loss of habitat cannot be reclaimed or fully restored to historic structure and function in the near future, and thus represents a constant reminder of the importance of the ongoing management of the remaining wetlands throughout the United States [79].

The amount of direct physical alteration can be estimated by monitoring the distribution of turbidity, suspended solids, each of which is coupled with physical processes, including tidal activity and wind forcing in the Blackbird Creek, where farming and agriculture practices may generate considerable runoff of fertilizers and pesticides [115]. The strength of hyperspectral data analysis techniques lies in their ability to provide both spectral and spatial views of surface water quality parameters that are typically not possible from in situ measurements. Hyperspectral Airborne Imaging Spectroradiometer for Applications (AISA) airborne sensors with high spectral and spatial resolution can be used for monitoring environmental changes in optically complex turbid environments.

Hyperspectral remote sensing has the potential to provide accurate synoptic views of water quality conditions over a large spatial extent, particularly the spatial distributions of total suspended solids (TSS) and phytoplankton that can be retrieved using remotely sensed data. This technique was applied in Blackbird Creek. Our second goal was to develop a procedure for the total suspended solids, turbidity, and total chlorophyll-*a* using method of hyperspectral data (Salem et al. unpublished data) [116]. Those characteristics were used to develop models

http://dx.doi.org/10.5772/66620

to map water quality characteristics in optically complex waters. Airborne AISA images with high spatial and spectral capabilities were used in a spectral analysis processes. The spectral angle mapper (SAM) classifier model was applied to AISA data to map spatial distribution of total suspended solids, chlorophyll-*a*, and turbidity levels. Photographs were used for results validation. The spectral analysis of wavelengths provided information on the distribution and concentrations of turbidity and Chl-*a* in Blackbird Creek.

Value increases in water quality parameters such as chlorophyll-*a*, turbidity, total suspended solids, and nutrients are symptomatic of eutrophic conditions. Concentrations of total suspended solids, chlorophyll-*a*, and turbidity parameters can provide insight on the extent of eutrophication and the potential impact on aquatic biota and overall water quality. Suspended solids may serve as a surrogate contaminant in agricultural watersheds since phosphorus, pesticides, and metals adhere to fine sediment particles and can be suspended in tidal estuaries. Estuaries receive continuous inputs of biogeochemical constituents from their fresh water sources and nutrients can be measured by monitoring water quality by estimating distributions of those materials [117]. There is a strong relationship between nutrient input, temperature, and phytoplankton biomass [118] but long-term monitoring of this relationship over a large scale provides information necessary for resource managers. Monitoring changes and impacts of land-use activities using remote-sensing technology provides the amount of data and information resource managers need to prepare management plans and policies for the watersheds.

The relationships between the spectral features of water reflectance and water quality parameters were investigated in Blackbird Creek. The research objective was to establish an empirical model that could be used for retrieval of water quality parameters from airborne hyperspectral AISA data in the Blackbird Creek Watershed. Hyperspectral AISA data provide a rapid and effective water quality-monitoring technique over a large spatial area for effective management of the watershed. Remote-sensing-monitoring results were coupled with the field-testing results. Four years of water quality-monitoring data from Blackbird Creek provided insight in relation to the land-use practices, especially agricultural activities in the watershed, and the presence of invasive *Phragmites*. Flyover photographs of the creek were taken from a small Delaware State University aircraft to help select locations in this research. Areas susceptible to sediment loads and chlorophylls were identified. This also allowed ground truth validation. Previous research by [119] provided the best fit spectral reflectance between 700 and 800 nm for total suspended solids. The scattering peak at ~700 nm was found to be strongly correlated with TSS and turbidity by Härmä et al. [120], Senay et al. [73], and Ammenberg et al. [121]. The image used includes 35 bands from 440 to 865 nm in the visible and infrared wavelengths in this research.

Aircraft-mounted hyperspectral spectrometer, the airborne imaging spectroradiometer for applications, was used to collect landscape images with 35 bands in Blackbird Creek. This type of spectroradiometer mounted in small aircraft can collect landscape images with a high spatial of 3.00 m × 3.00-m pixel size and a spectral resolution of 225 bands. Three segments of AISA images were selected to create a spectral library for phytoplankton (chlorophyll-*a*) in tidal water with high turbidity in the estuaries such as Blackbird Creek (**Figure 11**). Representative spectra for total suspended solids and chlorophyll-*a* in turbid water were

selected in the visible and near infrared region (NIR) for areas with similar characteristics. These types of spectral signatures are very useful in either small or large water bodies to monitor chlorophyll concentration (heavy, moderate, or light). AISA data were also used to measure water turbidity in Blackbird Creek and how this related to the primary productivity other than clarity of water. According to Ritchie and Cooper [93], AISA provides a better set of spectral bands in different wavelengths than what Landsat can provide. The spectral angle mapper classification model was used to monitor chlorophylls and total suspended solids based on its chemical composition using spectral signatures for each component (Salem et al. unpublished data) [116].

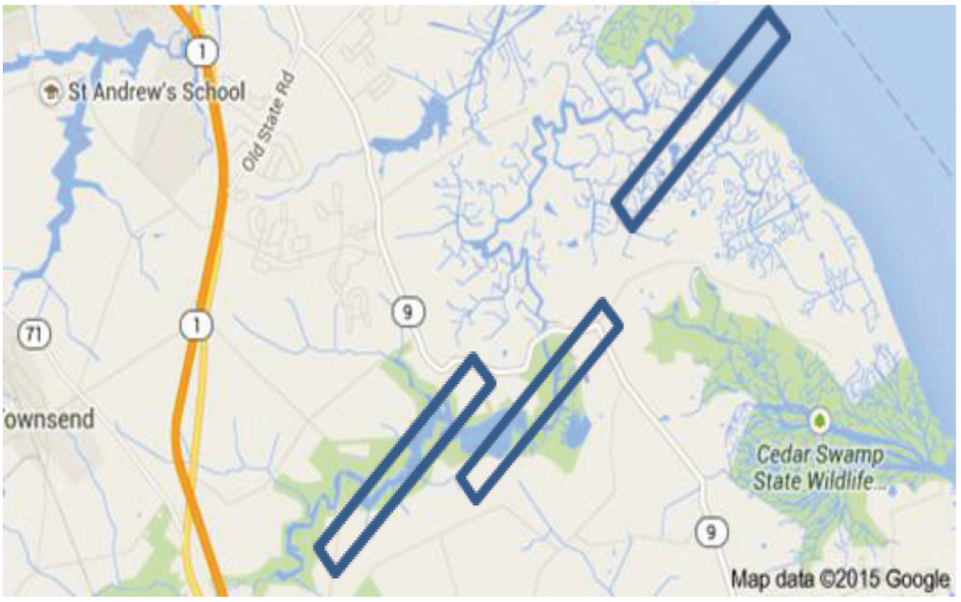

Figure 11. The three segments of AISA data used in the Blackbird Creek and Delaware Bay (Salem et al. unpublished data) [116].

The reflectance spectra of water with high chlorophyll concentration showed the characteristic absorption at the blue (~400 to ~500 nm) and red (~600 to ~680 nm) wavelength regions, which results in low reflectance, especially at ~680 nm wavelength (see **Figure 12**). Also, there is a phytoplankton-scattering peak at ~700 nm; this could be the result from a combination of chlorophyll fluorescence and water absorption at wavelength longer than 700 nm. The TSS reflectance appeared in all wavelengths from ~430 to ~860 nm, but TSS reflectance increases in clear water more than turbid water in the infrared range of the spectrum, and reflectance decreases in the infrared range due to high absorption of light by sediments in turbid water. Turbid water dominated the spectra on the visible (VIS) range of the spectrum, the high reflectance of total suspended solids appeared between (~460 and ~680 nm) and the sediments absorption of light appeared in the infrared portion between 680 and 860 nm which shows that sediments in turbid water absorb light in infrared range and reflect it on the visible range. The algae bloom spectra in turbid water show that chlorophyll absorption of light of phytoplankton bloom has no effect in the signatures taken away from the shoreline due to high turbidity which reduce the absorption effect of chlorophyll.

http://dx.doi.org/10.5772/66620

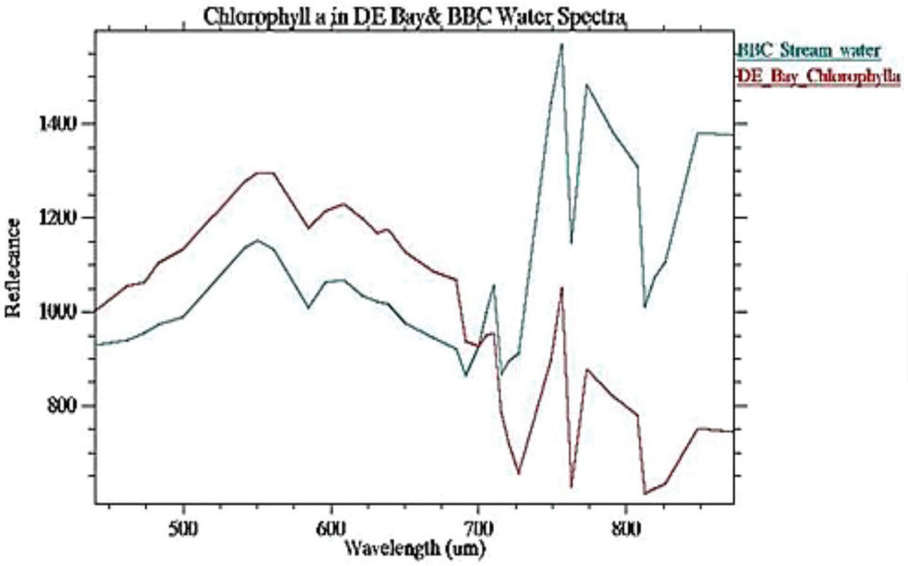

Figure 12. Spectral reflectance of chlorophyll and turbid water on the Blackbird Creek (BBC) and Delaware Bay (Salem et al. unpublished data) [116].

The signatures selected from the image of Blackbird Creek appeared in blue in **Figure 12** show low reflectance in the visible range of the spectra between (430 and 684 nm) due to absorption effect of the blue-green through red light of Chl-*a* and also show high reflectance of TSS reflectance in the near infrared range (727–813 nm) due to less turbid water in the Blackbird Creek than in the Delaware Bay. Low turbid water results in high absorption effect of chlorophylls in the visible range but low reflectance effect of TSS in the infrared range of the turbid water spectrum selected from Blackbird Creek.

Figure 13 shows classified image of different levels of suspended solids in the Blackbird Creek where high concentration of total suspended solids in relatively clear water is shown in the red color and vegetation in green color. The red signature in the spectral collection showed very high water reflectance and low impact on Chl-*a* absorption in the visible range from 430 to 680 nm because low turbid water increases the reflectance in the infrared range between 710 and 860 nm. The reflectance in yellow shows high absorption of Chl-*a* due to relatively clear water. Suspended solids and Chl-*a* show more increase in reflectance and absorption features because of less turbid water.

Results by Salem et al. (unpublished data) [116] indicated that high turbidity influences spectral reflectance scattering at ~700 nm of suspended solids, masking the spectral absorption of Chl-*a* due to the effect of high total suspended solids. These results reveal a positive correlation between water clarity and Chl-*a* concentration with the reflectance troughs caused by chlorophyll absorption at ~680 nm. This case study has demonstrated the feasibility to estimate the relative Chl-*a* levels and total suspended solids concentrations in the Delaware Bay and Blackbird Creek with limited ground-truthing data available (Salem et al. unpublished data). Through the use of remote sensing, hyperspectral imagery analysis combined with aerial photographs of the area and a general understanding of the conditions in the region can be estimated by monitoring relative Chl-*a* levels and total suspended solids concentration in applications of water quality management and policy decision.

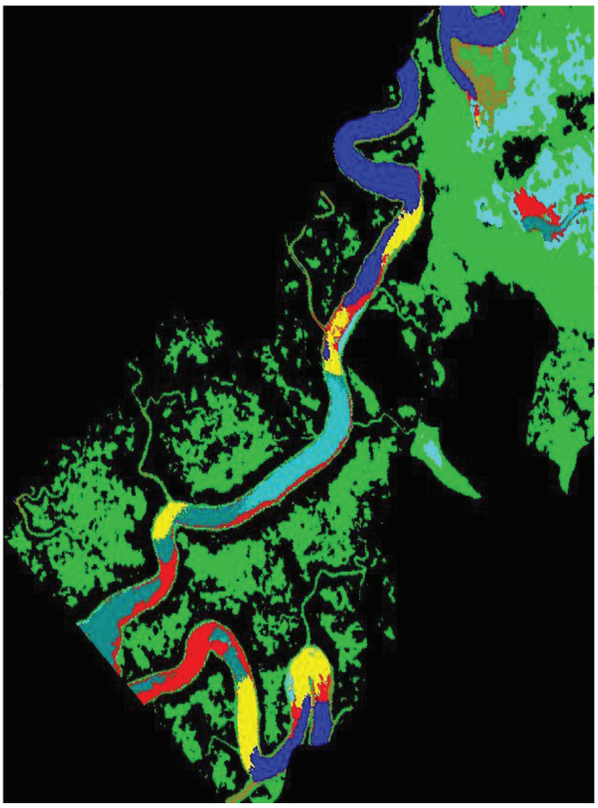

Figure 13. Classified image shows TSSs in red and vegetation in green and different levels of TSSs concentration are shown (Salem et al. unpublished data) [116].

2.3. Hyperspectral remote sensing of phytoplankton taxonomy in estuarine waters

Harmful algal blooms (HABs) have been observed to occur throughout the marine and aquatic environments of Earth during many different seasons, and under widely differing physical/chemical conditions. These blooms involve individual organisms which range in size from m*icroplankton (>20 μm), large nanoplankton (8–20 μm), small nanoplankton (1–8 μm), and picoplankton (<1 μm)* [122]. HABs are not known to have simple, direct correlations with location, seasonality, temperature, salinity, pH, insulation, nutrient concentrations, or other broadly collected physical oceanographic data [123]. Given the increasing number of occurrences of HABs in economically significant waters of the world, methods to be developed for early detection of the predominant type of bloom organism, which when used with other environmental and historic data, can alert authorities of a potential HAB versus a benign bloom condition.

Normally, the study of HABs is conducted by boats and point sampling, which is time consuming, expensive, and limited in spatial scale. Conversely, remote sensing has the capability of acquiring synoptic, regional-scale information, and is the only available technique that combines the possibility of frequent, large spatial coverage [124, 125] at reasonable cost. Ocean color imagery and products, from space-borne instruments such as Coastal Zone Color Scanner (CZCS) on Nimbus-7, Sea-viewing Wide Field-of-view Sensor (SeaWiFS) on board OrbView2, MODerate Resolution Imaging Spectrometer (MODIS) on EOS Terra and Aqua satellites, and the Medium-Resolution Imaging Spectrometer (MERIS) on ENVISAT, have

been used to study ocean surface phenomena for many years [126–129]. Most of these sensors focused on the detection of chlorophyll-a, the pigment common to all algae [130].

The techniques required to identify and quantify algal taxonomic composition are typically by time-consuming cell counts or more recently by high-performance liquid chromatography (HPLC) [131]. Many algae have accessory pigments that are taxonomically specific. Therefore, the detection of specific accessory pigments can often reveal the taxonomy of algae present in the aquatic system [132, 133]. Furthermore, each individual pigment has its own light absorption spectral features, so the detection of these optical features by remote sensing can discriminate the pigments and thus allow determination of the algal taxonomic composition. However, most of the sensors currently in ocean remote sensing cannot detect the algal accessory pigments because of a small number of spectral bands, that is, eight bands for SeaWiFS, six bands for MODIS, and the wide bandwidth associated with these limited numbers of spectral bands. Therefore, increasing the spectral resolution is critical to improve the capability of discriminating different algal groups by remote sensing. An (hyperspectral) imaging spectrometer is often defined as an instrument composed of numerous, contiguous, narrow spectral bands used to identify a material by its unique spectral features, and is the instrument of choice to identify algal groups as an imaging spectrometer.

Another challenge of remote sensing of algal blooms and HABs is the optical complexity in coastal and estuarine waters. Previously, most of the remote-sensing studies were focused on offshore case 1 waters (clear oceanic water, those waters whose optical properties are determined primarily by phytoplankton (Chl-*a*) and related colored dissolved organic matter (CDOM) concentration and detritus degradation products) where optical properties are fully determined by phytoplankton populations (phytoplankton and bacterial plankton) and their retinue (associated detrital material and CDOM), which are well correlated with concentrations of chlorophylls. This is in contrast to coastal Case 2 waters (waters whose optical properties are significantly influenced by other constituents such as mineral particles, CDOM, or microbubbles, whose concentrations do not correlate with phytoplankton concentration), where other substances, for example, sediments and dissolved materials, bottom features, also influence radiation propagation [134, 66]. Studies on the biogeochemistry in the coastal regions using satellite sensors are lacking due to the optical complexity of the coastal environment and sensor characteristics. Darecki et al. [135] studied the optical characteristics of two contrasting case 2 waters and their influence on ocean color remote-sensing algorithms, and concluded that, for accurate determination of chlorophyll from satellite-borne sensors in different coastal waters, a wider choice of spectral bands than currently available was needed.

Hyperspectral remote sensing better defines spectral signatures and provides more independent information to potentially resolve simultaneously phytoplankton, suspended matters, CDOM, and bottom contributions [136]. As discussed previously, multi-spectral remote-sensing instruments that measure chlorophyll-*a* concentration are valuable in determining the bloom distributions and variability of chlorophyll in the case 1 waters. To identify the dominant algal group of a bloom, it is necessary to quantify the absorption features by accessory or marker pigments beyond chlorophyll-*a* [137]. Hyperspectral measurements can resolve spectral features that are relatively narrow, such as those of the accessory pigments, and therefore

provide the possibility of identifying phytoplankton by taxonomic groups. Phytoplankton pigments, chlorophyll fluorescence, and in situ absorption spectra have been combined in studies to characterize micro-algal properties [138–142].

A number of research groups have used in situ or laboratory-based instruments to study the spectral properties of specific HAB groups in recent years. Millie et al. [140] demonstrated the utility of using bio-optical parameters for detecting and characterizing HABs by studying the photosynthetic pigments of *Gymnodinium breve*, a red tide dinoflagellate frequently appearing in Florida Bay. They concluded that the hypothetical assemblages of *G. breve* with increased concentration can be discerned from the absorption and the fourth-derivative information; however, the absorption spectra and the fourth-derivative alone may not identify the contribution of a chlorophyll c-containing taxon to the composite spectrum of a mixed assemblage. Richardson and Kruse [143, 144] were also successful in separating major types of algae and other parameters in Florida Bay using an AVIRIS imaging spectrometer.

To characterize the bio-optical properties of the coastal regions, the U.S. government has funded field campaigns to collect large suites of measurements from instruments based on numerous platforms: airborne, shipborne as well as in situ instruments. Those related to hyperspectral technology include HyCODE (Hyperspectral Coupled Ocean Dynamics Experiments) funded by the Office of Naval Research (ONR) [145, 146] and CICORE (California Center for Integrative Coastal Observation, Research and Education) funded by NOAA, NSF, and ONR. These campaigns with their large databases provide scientists with possibilities to study coastal ecosystems as never before. Although these field efforts were not specifically designed to "catch" the HABs' formation, maintenance, and dissipation, they help to build the bases for science and technology advancements in coastal region research including HAB studies.

In order to study the ecology of HABs and to address HAB forecast, detection, monitoring, and mitigation, a systematic effort is needed to develop methodologies that can be used uniformly for all types of HABs. Detecting the taxonomic grouping of phytoplankton is the initial step in identifying those classes that are harmful per geographic region. This information ultimately leads to managers and the public being accurately informed in terms of ecological and health issues. The bio-optical properties of the algal groups and the subsequent development of remote-sensing algorithms help by connecting laboratory and in situ studies with remote-sensing technology. These retrieval algorithms can further be incorporated into future operational satellite-monitoring systems to monitor specific taxonomic characteristics of HABs.

During a hyperspectral flyover mission supported by NOAA Environmental Cooperative Science Center (ECSC) in the Chesapeake Bay region in July, 2005 (**Figure 14**), over 20 GB of airborne hyperspectral imagery data were collected using the AISA (Airborne Imaging Spectrometer Applications)-Eagle hyperspectral scanner on an aircraft (Piper Saratoga, owned and operated by the University of Nebraska-Lincoln) at an altitude from 1525 to 3050 m, which provides 1- to 3-m spatial resolution for the target areas. The spectral range for the AISA-Eagle scanner is 400–1000 nm, and is programmable with regard to the number of individual spectral bands. The AISA-Eagle is a push-broom sensor with minimal smile and keystone. The hyperspectral data consisted of 95 discrete channels with band resolution of 2.5-nm full width at half maximum (FWHM) from the spectral range of 400–1000 nm.

http://dx.doi.org/10.5772/66620

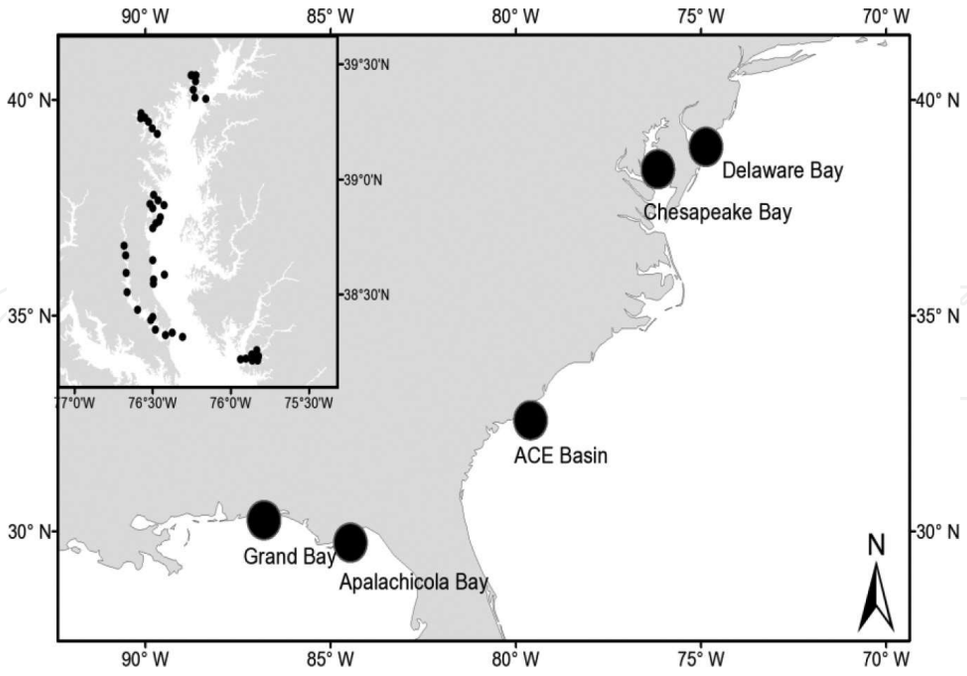

Figure 14. Map of the five estuarine systems located on the east and south coasts of US where the bio-optical data were collected from 2002 to 2008. The locations of each field station in the Chesapeake Bay observation from 2005 to 2008 are also shown in the upper left map [147].

The algorithms developed in the laboratory and field studies were applied to retrospectively analyze the aerial spectrometry imagery. The imagery was first atmospherically corrected using a recognized standard atmospheric correction program, FLAASH. Once the data have been converted into reflectance, further analysis was carried out using ENVI (the Environment for Visualizing Imagery, ITT Visual Information Solutions) software for algal population classification and biomass estimation. ENVI software includes a series of spectral analysis programs that can be used for such operations as locating the target spectra within the imagery by comparison with library of known spectra (end-member spectra) for specific algal groups. The results from imagery analysis were further compared to the ground-truthing data, which verifies the results of imagery analysis and further refines the approach for detecting HABs by hyperspectral remote sensing.

The results by Fan and Warner [147] show that the estuarine environment is optically complex, and chlorophyll, suspended sediments, and CDOM all influence the water reflectance. Chlorophyll-*a* has a prominent absorption trough near 675 nm, and the depth of the trough could be indicative of chlorophyll-*a* concentrations. High sediment concentration increases overall reflectance and amplifies pigment absorption features. The high CDOM concentration suppresses reflectance in the visual spectral range.

The Environment Cooperative Science Center (ECSC) data show no correlation between chlorophyll-*a* concentration and R490/R555 ratio [148]. An empirical algorithm was developed to more accurately predict chlorophyll-*a* concentrations in estuarine waters using hyperspectral remote sensing. The wavelength of chlorophyll-*a* absorption (675-nm band), the wavelengths sensitive to chlorophyll-*a* (650- and 700-nm bands) absorption, as well as the wavelengths

reflecting the effects of CDOM (550-nm band) and other suspended sediments (440-nm band) were included in this model. This algorithm can account for 72% of the variance in the chlorophyll-a data across a large area of estuarine waters, a considerable improvement compared to the previous algorithm (**Figure 15B**). By using the NIR region of the spectrum (600–750 nm), our attempts to estimate chlorophyll-*a* concentration, as well as the ability to filter out the effects of suspended sediments and CDOM, are promising.

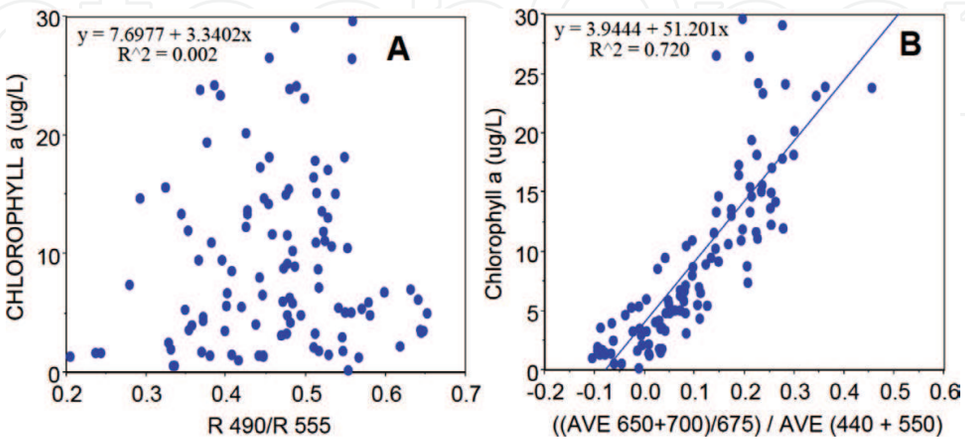

Figure 15. (A) Plot of the relationship between the model (R490/R555) and Chl-*a* concentration (μg/L) data collected across ECSC study sites; (B) plot of new algorithm (Ave (R650+R700)-R 675)/(Ave R440+ R550) versus Chl-*a* concentration (μg/L) collected across ECSC study sites [149].

Overall, our data suggest a great variability of optically active constituents (e.g., Chl-*a*, TSS, and CDOM) among the different estuarine systems, as well as the different field stations within a single estuarine system (**Figure 16**). The correlation analysis further indicates that the optically active water constituents are not related to each other (**Figure 16**) in this study. The determination coefficient ($R2$) of linear relationship between Chl-*a* and TSS is less than 0.01, suggesting that TSS and Chl-*a* did not co-vary together, and the major sources of TSS in the estuarine systems in this study might be from the land runoff. Similarly, no correlations were observed for concentrations of TSS and Chl-*a* versus CDOM absorbance, suggesting that the complex origins of these water optically active constituents, and phytoplankton (e.g., Chl-*a*) are not the only driver controlling the water optical properties.

The water reflectance $R(\lambda)$ (**Figure 17A**) measured in this study also displayed a large variation both in magnitude and in shape over the visible and NIR spectral regions. This variability is the direct result of largely uncorrelated optically active water constituents with various concentrations.

A common spectral pattern as shown in **Figure 17B** suggests that most of the spectra have a reflectance peak around 570 nm. This reflectance peak should be the results of the minimal absorption by Chl-*a* and the backscattering by particulates, such as TSS. A secondary reflectance peak was observed at red/NIR spectral range around 695 nm; this peak could be the result of Chl-*a* absorption at 675 nm and the strong water absorption at wavelength longer than 700 nm. Also, as shown in **Figure 17B**, the standard deviation of reflectance had similar pattern as the mean of reflectance, and it is wavelength dependent with a larger variance at the green spectral region.

http://dx.doi.org/10.5772/66620

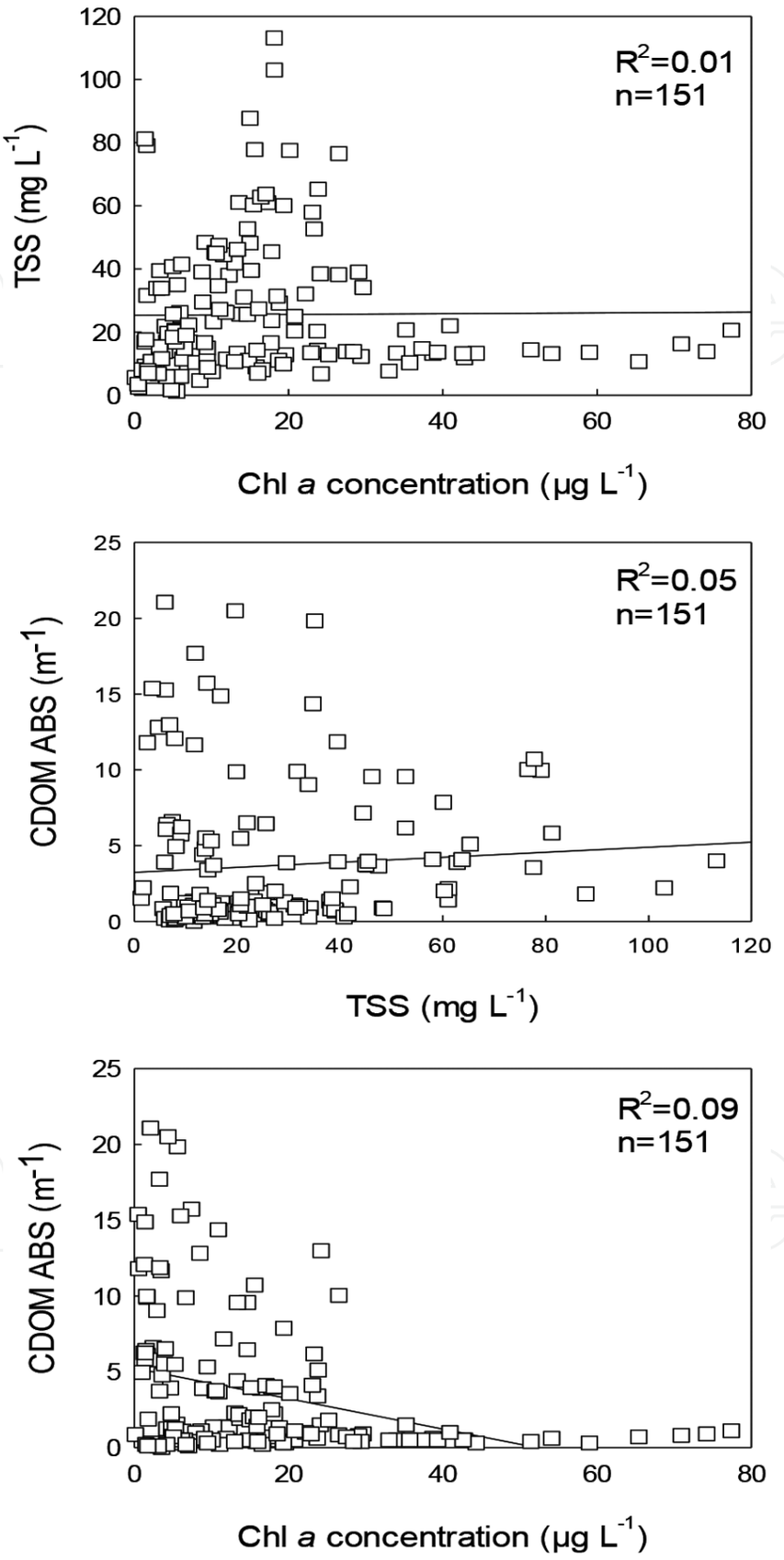

Figure 16. The relationships of bio-optical properties (e.g. Chl-*a* concentration, TSS concentration, and CDOM absorbance) of 151 field stations [147].

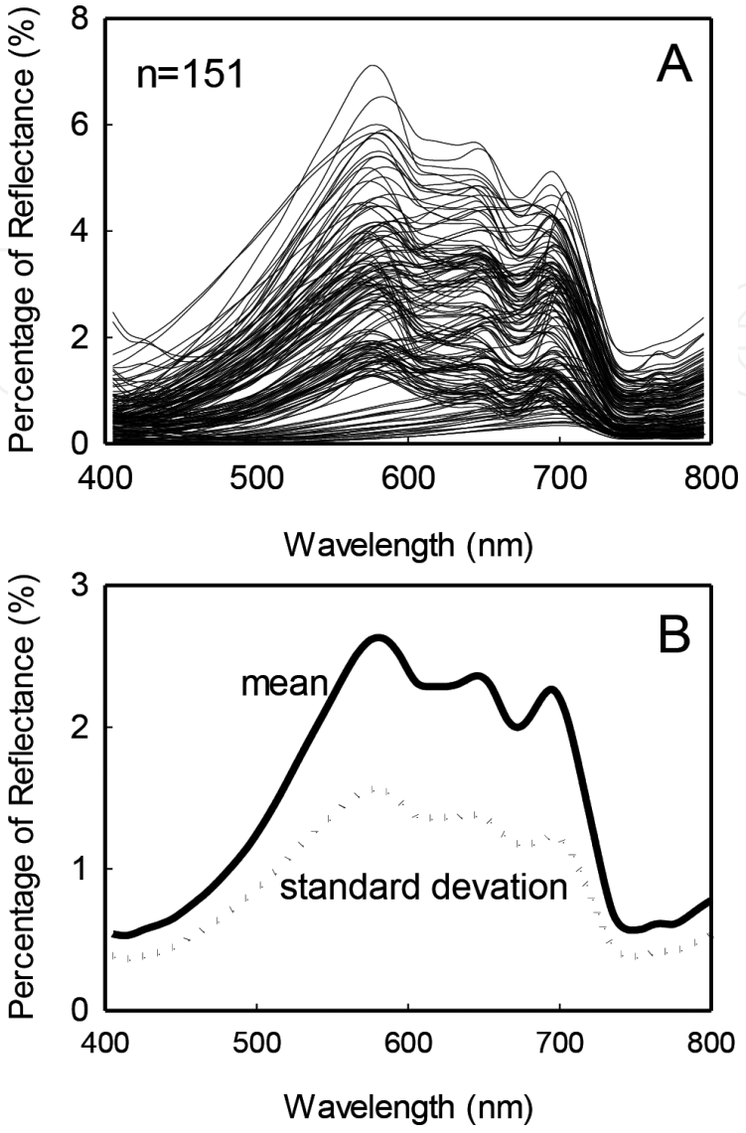

Figure 17. (A) Water reflectance $R(\lambda)$ spectra measured at 151 field stations from five estuarine systems on the east and south coasts of US; (B) the mean and standard deviation of the spectra [147].

A principal component analysis (PCA) of the reflectance dataset yields three dominant principal components which represented more than 97% of the total variance of the in situ water irradiance reflectance $R(\lambda)$ in our study (**Figure 18**). The first principal component accounts for 72.8% of the total variance, and displays the positive loadings across all wavelengths. Its spectral pattern is similar to the mean water reflectance observed in **Figure 17B**. This similar pattern suggests the backscattering by suspended particles controlling the overall water reflectance $R(\lambda)$. The second principal component accounts for 20.4% of total variance in the dataset. Its spectral shape was negative in blue and green spectral regions, with the minimal loadings around 560 nm. This feature corresponds to the minimal absorption by phytoplankton (e.g., Chl-*a* absorption) at this spectral range. Furthermore, the positive loadings in the red and NIR region could be contributed to the Chl-*a* absorption at 675 nm as well as the water absorption at this spectral range. So, the second principal component could be described as the effects of Chl-*a* (phytoplankton populations) absorption on water reflectance.

http://dx.doi.org/10.5772/66620

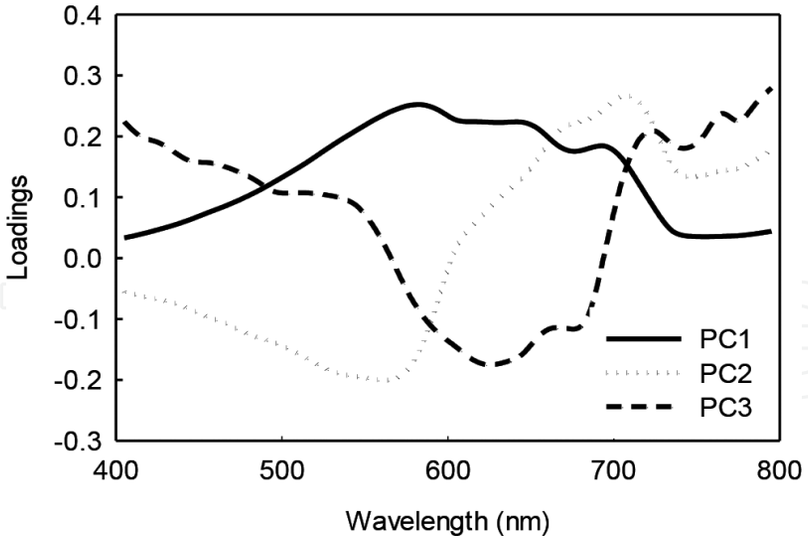

Figure 18. The loadings of the first three principal components of the correlation matrix of the reflectance $R(\lambda)$ dataset. The figure illustrates the weights by which the original spectral bands are weighted to construct the first PCs.

Figure 19 shows the biplot of the first two axes from canonical correspondence analysis (CCA), and it shows how the water reflectance in different in situ stations is influenced by water optical constituents (OACs), for example, Chl-*a*, TSS, and CDOM. The influences of OACs are indicated by vectors whose directions describe the gradients and whose lengths are proportional to their importance. While both TSS and CDOM have significant ($p < 0.01$) effects on first spectral axis, Chl-*a* has significant correlation ($p < 0.01$) with second spectral axis and nearly perpendicular to the TSS-CDOM gradient. So, the first CCA axis could represent the backscattering of the water, and TSS will increase the backscattering, while CDOM will suppress it. The second CCA axis could represent the influence of Chl-*a* (phytoplankton) on water reflectance. Together, these two axes explain most of the variability (96%) in the reflectance dataset.

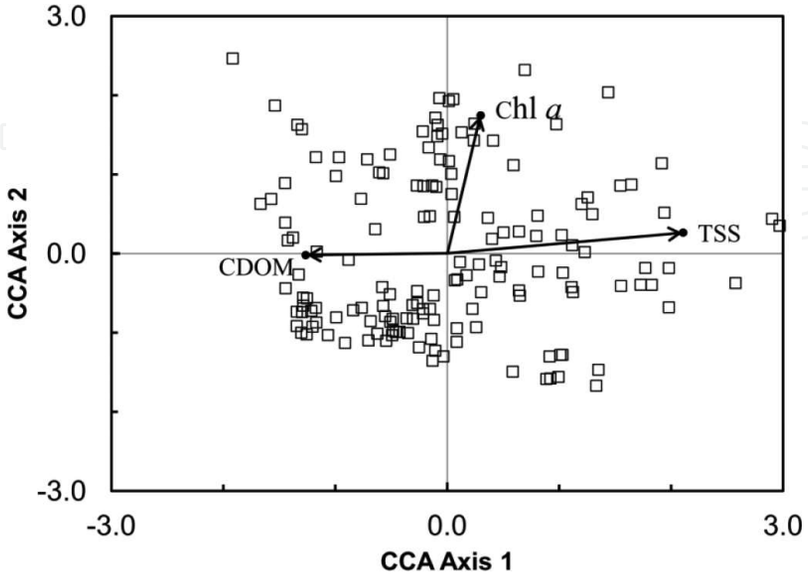

Figure 19. Biplot of the first two spectral axes of canonical correspondence analysis and the field stations. The influence of Chl-*a*, TSS, and CDOM is indicated by the vectors on this biplot [147].

This research advanced the basis of hyperspectral remote sensing under the optically complex coastal waters. The results provided necessary scientific information for using hyperspectral remote sensing in coastal and estuarine waters to monitor algal blooms. It also provides information leading toward the identification of the predominant bloom organism in estuarine waters. Knowing the type of organism as well as the synoptic view is of critical importance for coastal managers in their decisions relating to blooms, as well as being a more timely and economic method for this determination.

2.4. Spectral analysis of water reflectance for hyperspectral remote sensing of water quality in estuarine waters

Although hyperspectral remote sensing offers an effective approach for frequent, synoptic water quality measurements over a large spatial extent, the optical complexity of brackish estuarine water makes water quality monitoring by remote sensing a challenge. The third goal was to develop algorithms for hyperspectral remote sensing of water quality based on in situ spectral measurement of water reflectance [150].

During a hyperspectral remote-sensing study in the Chesapeake Bay, water reflectance spectra $R(\lambda)$ and the discrete water samples were collected at 11 field stations from 2008 to 2011 in the Patuxent River, a tributary of Chesapeake Bay (**Figure 20**). In this study, the relationships between the water reflectance $R(\lambda)$ and water quality parameters were examined to establish empirical algorithms that could be used for retrieval of water quality parameters from airborne hyperspectral data for rapid and effective water quality monitoring.

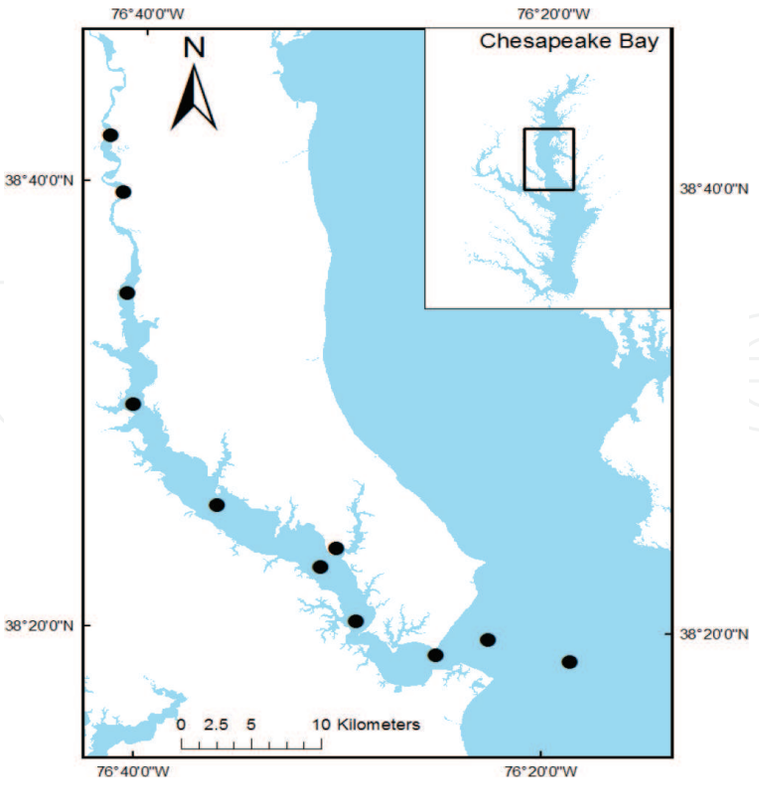

Figure 20. Map of the study area and the locations of the field stations for *in situ* measurement on the Patuxent River. The location of the study area in Chesapeake Bay watershed is shown in the upper right map [150].

http://dx.doi.org/10.5772/66620

Also, the aerial hyperspectral imagery of the Patuxent River with 2-m spatial resolution was acquired in the summer of 2005 using AISA-Eagle VNIR remote hyperspectral sensor (Center for Advance Land Management Information Technologies, University of Nebraska, Lincoln, NE). AISA-Eagle is a push-broom hyperspectral system with 1000-pixel swath width which can collect hyperspectral data at 2-m spatial resolution in 97 contiguous bands (2.5-nm bandwidth from 435 to 730 nm and 10-nm bandwidth from 730 to 950 nm). A total of six segments over a 50-km stretch of the Patuxent River were sampled during the summer of 2005.

The ground-truthing data suggest that water reflectance $R(\lambda)$ measured in this study displayed a high degree of variation because of the largely uncorrelated bio-optical properties. However, the influences on the general shape and magnitude of the reflectance by bio-optical constituents were still observed in this study. As shown in **Figure 21**, high chlorophyll-*a* concentration water shows characteristic absorption at the blue (400–500 nm) and red (600–680 nm) wavelength regions. Also, there is a phytoplankton-scattering peak at ~700 nm, which is the result from a combination of chlorophyll absorption and the strong water absorption at wavelength longer than 700 nm. This general influence on spectral reflectance by phytoplankton pigments (i.e., chlorophylls) is also consistent with our previous studies [147, 151]. Our data also suggest that TSS-dominated water shows high reflectance across a wide spectra range from 560 to 700 nm. This influence of TSS in regulating water reflectance spectra was also observed in the previous studies [152, 153]. For the water with high CDOM concentrations, its reflectance was characterized by low reflectance across the blue and green spectral regions, with very small reflectance peaks near 660 and 700 nm [151].

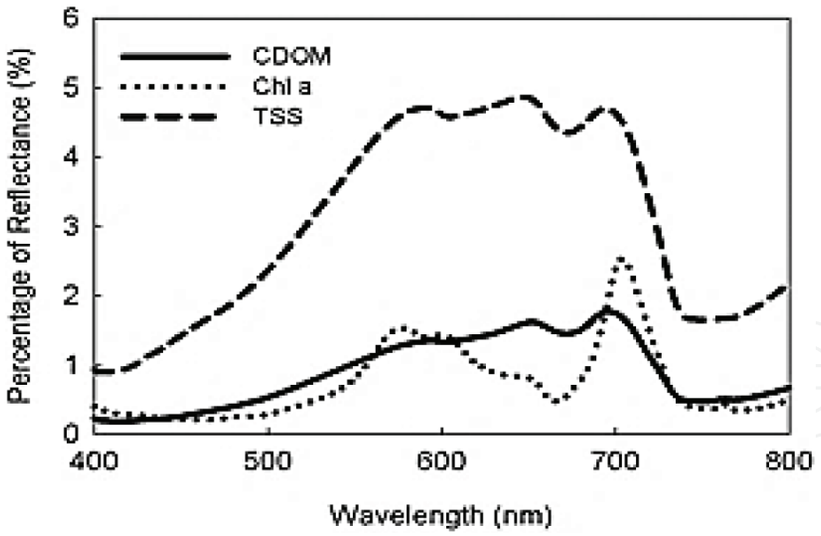

Figure 21. The general spectral features for coastal water that are dominated by high concentrations of Chl-*a*, TSS concentrations, and absorption of CDOM [147].

The general features of reflectance spectra observed in this study further provided insights for wavelength bands selection that are likely to be used for retrieval models to retrieve water quality parameters (i.e., Chl-*a*, TSS, and CDOM) [151]. Based on the in situ measurements in this study, band ration algorithms were developed to establish the relationships between water reflectance and selected water quality parameters, and this approach has been suggested as one of the most

appropriate methods elsewhere [154]. Several previous studies showed strong relationships between log-transformed water quality data and reflectance values from hyperspectral data [151].

Chlorophyll-*a* model: As one of the most commonly measured water quality parameters, Chl-*a* has a significant correlation with the reflectance ratio of 700–670 nm in our dataset (**Figure 22A**). This was also found to be the case in several previous studies [155]. This relationship is due to the backscattering by phytoplankton at 700 nm and the strong absorption at 670 nm. The regression model is of the following form:

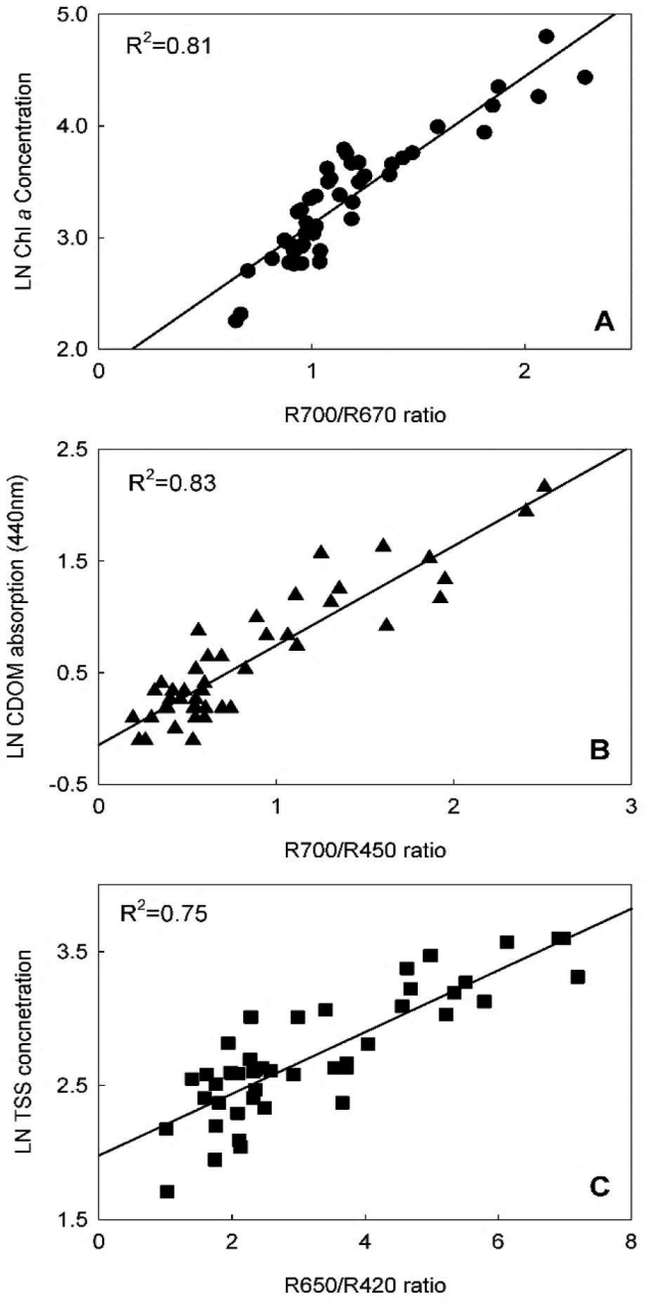

Figure 22. Scatter plots of *in situ* log-transformed water quality parameters versus corresponding band ratio values: (A) Chl-*a;* (B) CDOM; and (C) TSS [150].

$$LN(\text{Chl-}a) = 1.29\left(\frac{R700}{R670}\right) + 1.83, \quad \text{with } R^2 = 0.81 \tag{1}$$

CDOM model: Because of low CDOM concentration in lot oceanic areas, the impacts of CDOM on spectral variability have been largely neglected in some previous studies [156, 157]. This study shows that CDOM concentration strongly suppressed the reflectance at blue-to-green wavelength region, and then this effect declined exponentially toward the longer wavelength (**Figure 21**). Based on this CDOM spectral feature, the regression model (**Figure 22B**) was developed as the following form:

$$LN(\text{CDOM}) = 0.89\left(\frac{R700}{R450}\right) - 0.15, \quad \text{with } R^2 = 0.83 \tag{2}$$

TSS model: TSS represents both living organic solids (mainly phytoplankton) and inorganic suspended solids which mainly contribute to scattering of light. So, as shown in **Figure 21**, water with high TSS concentration tends to have high reflectance, especially at 500–600-nm regions. Remote-sensing algorithms for TSS reported in literature are less consistent and more dependent on the specific bio-optical conditions [158]. In this dataset, the relationships between log-transformed TSS concentration showed good correlation with the reflectance ratio of 650:420 nm. The regression model (**Figure 22C**) is of the following form:

$$LN(\text{TSS}) = 0.23\left(\frac{R650}{R420}\right) + 1.98, \quad \text{with } R^2 = 0.75 \tag{3}$$

Water quality mapping: The ASIA-Eagle hyperspectral imagery acquired in this study was processed and classified by using EXELIS ENVI 4.7 and ESRI ArcGIS 10.1. The ASIA imagery was first corrected geospatially and radiometrically to "at platform reflectance," then atmospheric correction was conducted on the image using the FLAASH in ENVI using the band at 820-nm wavelength to produce the image of "water reflectance." This "water reflectance" imagery is further classified by using a supervised classification in ENVI based on the selected water region of interests (ROIs). The terrestrial features were masked out to create the water-only image for further analysis. Finally, the band ratio models developed in this study were applied to these radiometric data in the image to create the pixel-level water quality maps. **Figure 23** shows the pixel-level maps of water quality (Chl-*a*, TSS, and CDOM) in a small section of the flight segment at the mouth of the Patuxent River. These maps clearly demonstrate the heterogeneity of water quality over a relatively small area. A patch of phytoplankton bloom (dinoflagellate *Prorocentrum minimum*, based on field observation) with high Chl-*a* concentration was observed in the middle of the river, while the Chl-*a* concentration in other area was relatively low. The water quality maps also show that the water with high TSS concentration was mainly located in the small creeks, coves, and river banks, suggesting that the land runoff might be the major source for TSS in water column. The CDOM absorption was also found high in the small creeks and coves around the river, as well as in the area with phytoplankton blooms. This suggests that the origin of CDOM could be both terrestrial or produced during the algal bloom.

Overall, the feasibility of hyperspectral remote sensing that can capture the fine-scale variation of water quality parameters is illustrated in **Figure 23**. In these maps, the algal bloom could be very patchy, and there was a large variation in these water quality parameters over a relatively small body of water. These techniques could provide vast water quality information

that would not be seen by conventional monitoring program which probably only involve several sampling stations in the same area. However, the retrieval models in this study were derived from the dataset that is specific to the study area, which do not necessarily represent the coastal waters in other areas. The accuracy of such algorithms is always subject to the location of ground-truthing dataset.

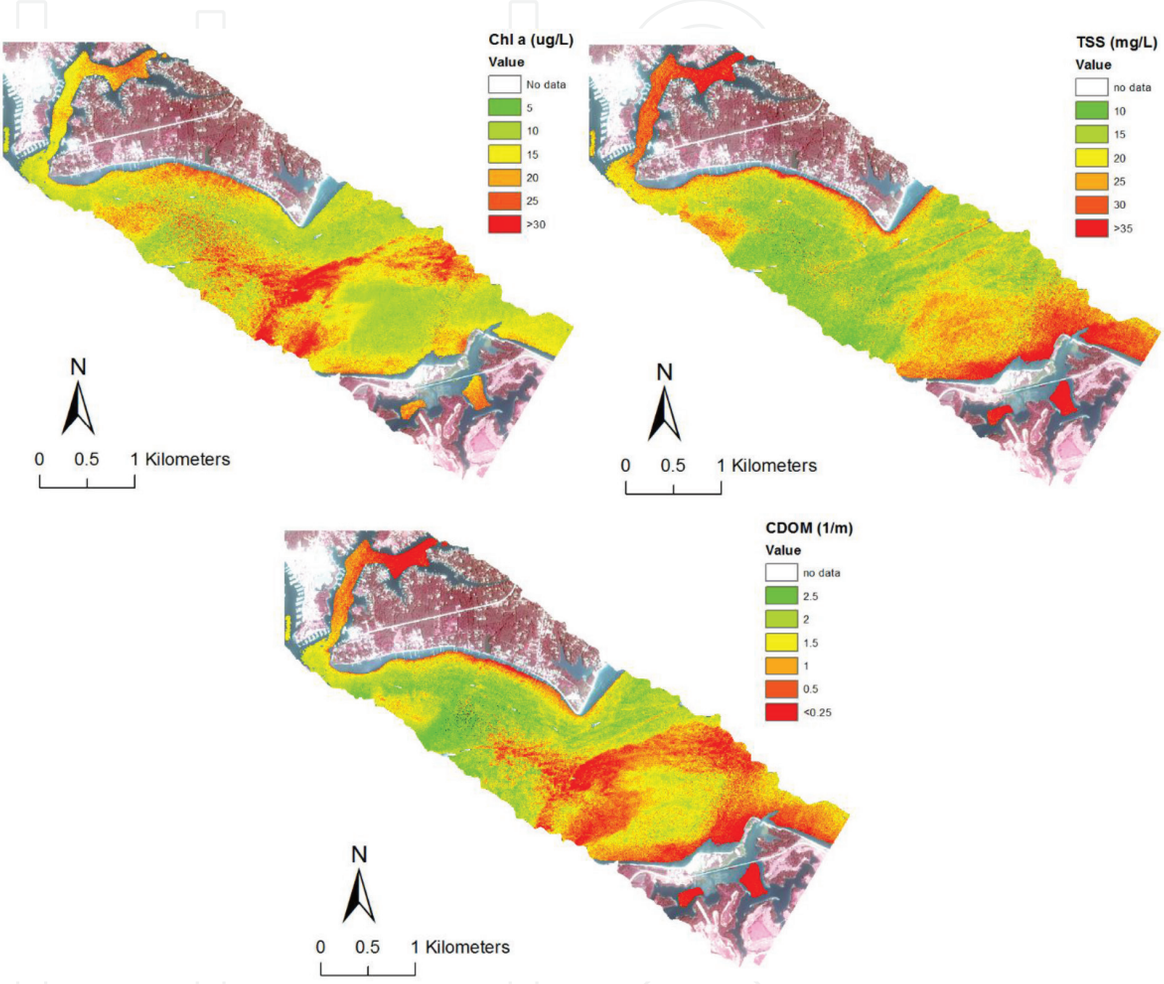

Figure 23. Maps of Chl-*a*, TSS concentrations, and CDOM absorption at the mouth for the Patuxent River, summer 2005 [150].

2.5. Estimating chlorophyll-*a* concentrations in the coastal St. Jones River Watershed using AISA images

The St. Jones River Watershed (**Figure 24**) is located in central Kent County, Delaware, and drains a portion of the coastal plain. The total area of the St. Jones River Watershed is 23,300 ha, including most of the capital city of Dover and a portion of Dover Air Force Base [157]. The upper St. Jones River is impounded by a dam 17 km upstream from the bay to form Silver Lake, a municipal recreation area. Much of the eastern portion of the watershed consists of wetlands, agricultural lands, and forests, including lands and waters managed for waterfowl, wild turkey, deer, and other wildlife.

http://dx.doi.org/10.5772/66620

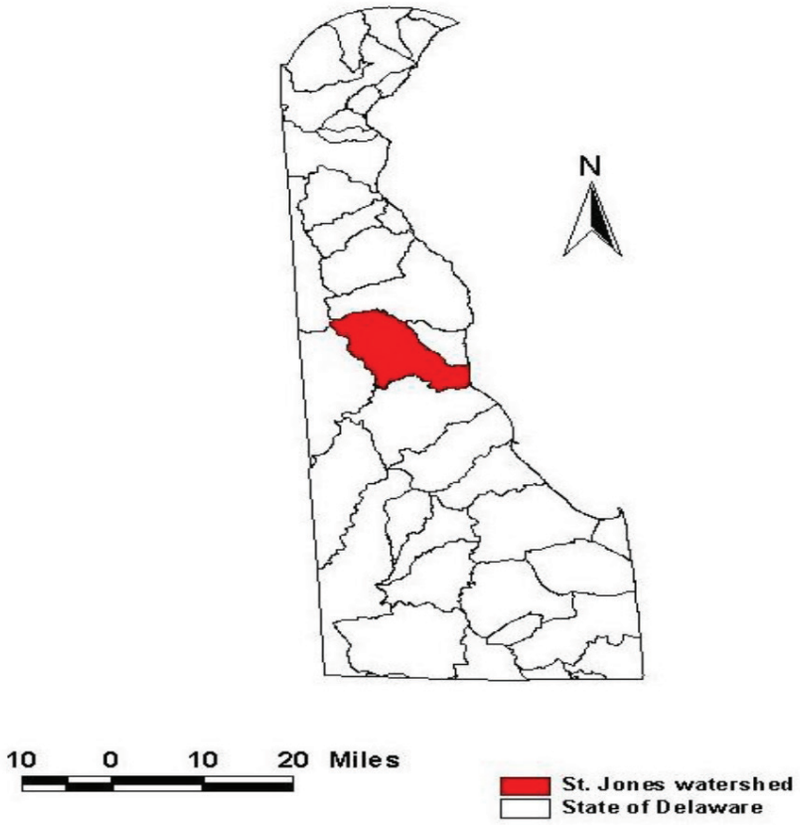

Figure 24. Location of the study watershed within the state of Delaware [158].

The percentage of various land uses in the St. Jones River Watershed in 1992 and 2001 was calculated based on the USGS land use/cover map of Delaware in 1992 and 2001, and there were significant changes in land use in the St. Jones River Watershed during this period (**Table 1**). While more lands were converted to urban and agricultural land, there was significant loss of wetland and open water in the St. Jones River Watershed. However, agriculture is always dominant land use in the St. Jones River Watershed at both time periods. Thus, it is important to examine chlorophyll-*a*, an indicator of eutrophication induced by agriculture runoff, in water bodies.

Land use	%, 1992	%, 2001
Open water	2.3	1.5
Urban	13.2	17.0
Forest	15.4	14.7
Agriculture	53.1	55.3
Wetland	15.7	10.8
Barren	0.3	0.7

Table 1. Percentage of land use in the St. Jones River Watershed in 1992 and 2001 [160].

In this watershed, eight water segments were in the 303 list for nutrients, dissolved oxygen (DO), and bacteria that were contributed from non-point sources (NPS) [19]. Many stations experience low DO levels less than the state minimum WQS of 4 mg/L with elevated chlorophyll-*a* levels. Also, nutrient concentrations at most of stations were high enough to support algal growth [19]. Therefore, it is essential to monitor chlorophyll-*a* concentrations in water bodies in the St. Jones Watershed.

The Airborne Imaging Spectrometer for Applications (AISA) is a commercially produced hyperspectral push-broom-type imaging spectrometer system capable of collecting data within a spectral range of 430–900 nm. The AISA airborne system, manufactured by Spectral Imaging (Finland), offers a high degree of positional accuracy provided by the combination of a differential global positional system (DGPS) with an integrated navigation system (INS) and real-time Kalman filter.

Aligned with the second goal in this chapter, this study determined if hyperspectral data could be used to measure water quality indicators such as chlorophyll-*a*, TSS, and CDOM in Delaware coastal waters. The correlation between a spectral index and in situ chlorophyll-a concentration was examined. Spectral indices were compared to determine the best index used for retrieval of chlorophyll-*a* from Delaware coastal waters with high confidence.

From July 20 to July 23, 2004, Delaware State University and the NOAA-sponsored Environmental Cooperative Science Center (ECSC) conducted a hyperspectral imaging flyover of the St. Jones River Watershed, Delaware. AISA data were acquired by the Center for Advanced Land Management Information Technologies (CALMIT) at the University of Nebraska using the AISA-Classic as the primary on-board sensor flown in a specially modified Piper Saratoga aircraft. The AISA sensor was configured for 35 spectral bands from 441 to 873 nm, and bandwidths varied for different portions of the spectrum. During the flyover, 25 flight lines (strips) of hyperspectral imagery were obtained between 11 AM and 2 PM covering the major parts of the St. Jones River Watershed. A ground resolution of 3.0 m was achieved by flying at an average altitude of 1500 m. One of the goals for this flyover was to determine if hyperspectral data could be used to measure water quality indicators such as chlorophyll-a, TSS, and CDOM in Delaware coastal waters.

Ground-truthing measurements included water sampling for laboratory analysis (chlorophyll-a, nutrients, and total suspended solids) and in situ measurement of water quality parameters including salinity, conductivity, dissolved oxygen, and temperature. Water samples were collected as close to the aircraft overpass as possible, with the exact coordinates of the sampling stations determined using a Garman GPS unit. All samples were taken from the 0- to 0.4-m surface layer. After acquisition, the AISA images were radiometrically and geometrically corrected by CALMIT using calibration files fed to AISA CaliGeo® Software and converted to Environment for Visualizing Images (ENVI) file format.

ENVI software (RSI, Version 4.2) was used to process preprocessed AISA images. AISA images for the study area and one shape file of sampling sites (GPS points) were loaded into ENVI. To reduce noise in the data, one 3 × 3 kernel window was used at each sampling site to extract spectral profiles, which include values for each band. Then, all spectral profiles were exported and input into Excel for further processing.

http://dx.doi.org/10.5772/66620

In Excel, NIR/Red "index" values were calculated based on different combinations of NIR and red bands, using one near infrared band between 670 and 780 nm and one red band between 620 and 670 nm. Fifty different NIR/red ratios were computed in total. Correlations between spectral indices and in situ chlorophyll-a data were examined and the significance of the correlations tested. If there was a significant relationship between an index and measured chlorophyll-*a*, the index was examined again to see if it had any significant relationship with measured TSS. The residual difference between estimated chlorophyll-*a* and measured chlorophyll-*a* was also tested to determine if there was a significant relationship between the residuals and measured TSS for each initially identified spectral index. This procedure was used to determine if TSS was potentially responsible for any estimate bias in the spectral indices. Based on all three procedures, indices that were a good fit for retrieving chlorophyll-*a* in Delaware coastal waters were finally identified.

Results are shown in **Table 2**. It shows all ratio indices possessing a significant relationship with in situ chlorophyll-*a*. There were significant relationships between chlorophyll-a and ratios covering near infrared bands only from 692 to 705 nm. Gitelson [159, 160] stated that reflectance near 700 nm was sensitive to chlorophyll-a in inland and coastal waters, and our result confirmed his finding.

Spectral indices	Correlation coefficients	Spectral indices	Correlation coefficients
R692/R621	0.56	R700/R651	0.53
R692/R632	0.55	R700/R670	0.58
R692/R639	0.57	R705/R621	0.50
R692/R651	0.56	R705/R632	0.49
R692/R670	0.68	R705/R639	0.50
R700/R621	0.54	R705/R651	0.49
R700/R632	0.53	R705/R670	0.52
R700/R639	0.54	R710/R670	0.47
SI	0.53		

Critical value (n = 16) = 0.47 at α = 0.05.

Table 2. Correlation coefficients between spectral indices and chlorophyll-a in the St. Jones River Watershed [160].

There was no significant relationship between the ratios and in situ TSS found. There was also no significant correlation between the residuals of estimated versus in situ chlorophyll-*a* and in situ TSS. These results demonstrated that TSS did not have significant impact on estimating chlorophyll-*a* in Waters in St. Jones River Watershed when using the indices identified from this study.

While significant, the correlation coefficients for sensitive spectral indices are not high (maximum R = 0.68). This may be caused by two reasons. First, there was a time gap between the time to collect AISA images and the time to obtain water quality samples. Second, no atmospheric correction has been performed on the AISA images in this study. Despite these limitations, significant correlations obtained from this study indicate that it is possible to monitor chlorophyll-*a* using AISA images in Delaware coastal water bodies.

Based on this study, some simple ratio algorithms using spectral bands in the red and red-edge ranges were adequate for quantifying chlorophyll-*a* in coastal waters. These algorithms were validated in other environments such as Nebraska with some modification to the coefficients [160]. Therefore, there is a high potential that chlorophyll-*a* in coastal waters could be estimated using hyperspectral remote sensing without the interference from TSS. NIR/red ratios covering red-edge bands from 692 to 705 nm were found to be useful for retrieving chlorophyll-*a* in Delaware coastal waters when using AISA images and they could work in similar situations in other coastal areas. This suggests the advantage of using ratio-based indices in estimating coastal chlorophyll-*a* concentrations by remote sensing.

3. Final remarks

The impacts of land use on aquatic health and marsh habitat have been a constant battle, and the rate of our wetlands lost is far more than they can be replaced. Tidal marsh ecosystems serve as great examples of dynamic ecosystems that can provide numerous lessons in restoration and management strategies. The ubiquitous incidence of aquatic species as both temporal and spatial perspectives indicates the importance of these types of systems to sustain the health of aquatic species and other important species in the face of anthropogenic and environmental stresses. Thus, it would be pertinent for managers to maintain the health of these areas by preventing any further alterations and damage, especially from nutrient runoff and abusive use of our coastal lands, and the invasion of *P. australis*.

The Blackbird Creek Watershed is composed of only 4% urban development. This provided a great opportunity to study the area that has very little anthropogenic impact, relative to other watersheds. How trophic dynamics can be affected as a result of various land uses is one of the concerns. There are several plots of land designated as cropland in Blackbird Creek. An understanding of crop rotation in these plots both within and between seasons can provide insight on whether changes in crops across years can affect trophic interactions and food web dynamics. Additionally, effectiveness of riparian buffers as blockades for fertilizer runoff is a significant impact on water quality. With sites associated with buffers and sites without buffers, different food web characteristics can be identified, especially if there are inconsistencies in the nutrient concentrations. While this is intriguing, it would be more beneficial if a second watershed with more urban areas and anthropogenic effects was used. The St. Jones Watershed is composed of over 21% urban development. If similar work can be done in each of these watersheds, we may be able to discern the effects of different land uses on Delaware's coastal waterways.

The Chesapeake Bay is under increasing pressures from anthropogenic disturbances at various temporal and spatial scales. Water quality monitoring is vital for assessing such impacts, and further provides important information for sustainable water resource managements. The research in this chapter demonstrates the applications of hyperspectral remote sensing in retrieval of the water quality parameters in such an optically complex system. Further development of retrieval algorithms is still needed in order for the remote sensing to be routinely used in the water quality monitoring.

Based on the studies discussed in this chapter, in almost every watershed studied, major land use and cover change are due to the conversion of agriculture land to developed land in the Mid-Atlantic region. Urban runoff has gradually become a dominate pollution sources to the natural environment, including wetlands and open water bodies. More attention needs to be paid to locate the position and size of land conversion in order to effectively manage and control urban runoff. Also, it is necessary to monitor the spread of invasive plants, especially *P. australis* and its impact on vegetation communities in coastal watersheds within the region. Hyperspectral images have advantages in accurate land classification and can keep track of detailed changes in land use and cover. This will help build more effective land management practices in Mid-Atlantic region.

All studies above reveal that it is feasible to measure water quality indicators including chlorophyll-*a*, TSS, and CDOM using hyperspectral images and simple spectral algorithms. These algorithms involve spectral bands in the red and red-edge ranges and they can capture unique spectral signatures of these water quality indicators such as chlorophyll-*a* in coastal waters. All studies suggest the advantage of using hyperspectral images in estimating chlorophyll a-concentrations, TSS, and CDO in various coastal water bodies. Future research focusing on the direct measurements of in situ inherent optical properties (IOPs) such as absorption coefficients and backscattering for different estuarine systems is needed to develop better algorithms for water quality retrievals which include TSS and CDOM by remote sensing in coastal waters. With application of remote-sensing technology, real-time data collection of water quality parameters and plant community changes for the entire watershed will help resource managers to develop better management strategies.

Acknowledgements

We would like to thank the following individuals for their assistance and support for research discussed and in preparation of this chapter: Matthew Stone, Kris Roeske, Laurieann Phalen, Morgan State University Patuxent Environmental and Aquatic Environmental Laboratory (PEARL) and Delaware State University Aquatic Sciences Laboratory team members for field assistance and the early comments and discussions on the research papers. The authors also thank Dr. Shobha Sriharan at the Virginia State University for her support and Delaware State University for providing support and resources to conduct the research in this chapter. Case studies provided in this chapter are funded in the following order:

Case Study 2.1 is funded by NSF EPSCoR Grant Award# EPS-1301765 and the USDA-NIFA CBG Grant Award# 2013-38821-21246 to the Virginia State University.

Case Study 2.2 is funded by USDA-NIFA CBG Grant Award# 2010-38821-21454 to the Delaware State University and USDA Evans-Allen Grant Award# DELXDSUGO2015.

Case Study 2.3 is partly supported by NOAA-ECSC Grant Award# NA11SEC4810001, the NSF Grant Award# GEO0914546 to the Morgan State University, and the NSF Grant Award#

1036586 to the University of Maryland Eastern Shore and the USDA-NIFA CBG Grant Award # 2011-38821-30892 to the Virginia State University.

Case Study 2.4 is partly supported by NOAA-ECSC Grant Award# NA11SEC4810001, the NSF Grant Award# 1036586 to the University of Maryland Eastern Shore, and the USDA-NIFA Grant Award# 2013-38821-21246 to the Virginia State University.

Case Study 2.5 is funded by NOAA-ECSC Grant Award# NA11SEC4810001.

Author details

Gulnihal Ozbay[1]*, Chunlei Fan[2] and Zhiming Yang[3]

*Address all correspondence to: gozbay@desu.edu

1 Department of Agriculture and Natural Resources, Delaware State University, Dover, DE, USA

2 Patuxent Environmental and Aquatic Research Laboratory, Morgan State University, Baltimore, MD, USA

3 Department of Environmental, Earth and Geospatial Sciences, North Carolina Central University, Durham, NC, USA

References

[1] NOAA National Ocean Service. 2016. What Percentage of the American Population Lives near the Coast? http://oceanservice.noaa.gov/facts/population.html (accessed 15 June 2016).

[2] Stone ML. 2016. Land Use Practice and Water Quality, Blue Crab Population Dynamics and Fish Biodiversity in Blackbird Creek, Delaware. Master's Thesis. Natural Resources Program, Department of Agriculture and Natural Resources, Delaware State University, Dover, Delaware. p. 103.

[3] Nehrling R. 2013. Fertilizer Use and Markets: USDA Website. http://www.ers.usda.gov/topics/farm-practices-management/chemical-inputs/fertilizer-use-markets.aspx (accessed 15 June 2016).

[4] NOAA National Ocean Service. 2008. Estuaries: Human Disturbances to Estuaries. http://oceanservice.noaa.gov/education/kits/estuaries/ estuaries09_humandisturb.html (accessed 15 June 2016).

[5] Fan C, Warner R, Lacouture R. 2011. Hyperspectral Remote Sensing of Phytoplankton Taxonomy in Estuarine Waters. Ecology and Oceanography of Harmful Algal Blooms (ECOHAB), EPA-G2008-STAR-A1. Proposal. p. 38.

[6] Simenstad CA, Tanner CD, Thom RM, Conquest LL. 1991. Estuarine Habitat Assessment Protocol. Report to U.S. Environmental Protection Agency, Region 10, Seattle, Washington. EPA 910/9/91/037. p. 201.

[7] Stribling JM, Cornwell JC. Identification of important primary producers in a Chesapeake Bay tidal creek system using stable isotopes of carbon and sulfur. Estuaries and Coast 1997; 20(1): 77–85. doi:10.2307/1352721.

[8] Weinstein MP, Balletto JH. Does the common reed, *Phragmites australis*, affect essential fish habitat? Estuaries and Coasts 1999; 22: 793–802. doi:10.2307/1353112.

[9] Meyerson LA, Saltonstall K, Windham L, Kiviat E, Findlay S. A comparison of *Phragmites australis* in freshwater and brackish marsh environments in North America. Wetlands Ecology and Management 2000; 8: 89–103.

[10] Windham L, Ehrenfeld JG. Net impact of plant invasion on nitrogen-cycling processes within a brackish tidal marsh. Ecological Applications 2003; 13(4): 883–896.

[11] Able KW, Hagan SM, Brown SA. Mechanisms of marsh habitat alteration due to *Phragmites*: response of young-of-the-year mummichog (*Fundulus heteroclitus*) to treatment for *Phragmites* removal. Estuaries and Coasts 2003; 26(2):484–494.

[12] Ozbay G, Augustine A, Fletcher R. Remote sensing of *Phragmites australis* invasion in Delaware tidal marsh zones: issues to consider. Journal of Geophysics and Remote Sensing. 2003. doi: 10.4172/2169-0049.100e107. doi:10.3368/er.28.3.254.

[13] Orson RA. A paleoecological assessment of Phragmites australis in New England tidal marshes: changes in plant community structure during the last few millennia. Biology Invasions 1999; 1: 149–158.

[14] Warren RS, Fell PE, Grimsby JL, Buch EL, Rilling GC. Rates, patterns, and impacts of *Phragmites australis* expansion and effects of Phragmites control on vegetation, macroinvertebrates, and fish within tidal wetlands of the lower Connecticut River. Estuaries 2001; 24: 90–107.

[15] DNREC. 2016. Delaware Private Lands Assistance Program. http://www.dnrec.delaware.gov/fw/dplap/services/LIP/Pages/PhragmitesFacts.aspx (accessed 15 August 2016).

[16] NERRS. 2009. National Estuarine Research Reserve System. St. Jones River Site Description. http://nerrs.noaa.gov (accessed 18 June 2016).

[17] Index Mundi. 2014. United States—Population Growth Rate (2010–2014) by State http://www.indexmundi.com/facts/united-states/quick-facts/all-states/population-growth#map) (accessed 15 June 2016).

[18] Delaware Watersheds, State of Delaware. 2016. Blackbird Creek. http://delawarewatersheds.org/the-delaware-bay-estuary-basin/blackbird-creek/ (accessed 15 June 2016).

[19] DNREC. 2006. Blackbird Creek Watershed proposed TMDLs. Report DNRE0080. p. 54. http://www.dnrec.delaware.gov/swc/wa/Documents/TMDL_TechnicalAnalysisDocuments/5_BlackbirdTMDLAnalysis.pdf (accessed 15 June 2016).

[20] Rabalais NN, Turner RE, Justic E, Dortch Q, Wiseman WJ, Gupta BKS. Nutrient changes in the Mississippi river and system responses on the adjacent continental shelf. Estuaries 1996; 19:386–407.

[21] Boesch DF, Brinsfield RB, Magnien RE. Chesapeake Bay eutrophication: scientific understanding, ecosystem restoration, and challenges for agriculture. Journal of Environmental Quality 2001; 30:303–320.

[22] The News Journal. 2014. Delaware's Broiler Chicken Output Grows. http://www.delawareonline.com/story/money/business/2014/04/29/delawares-broiler-chicken-output-grows/8475187/ (accessed 15 June 2016).

[23] USDA NASS. 2010. Delaware Agriculture. https://www.nass.usda.gov/Statistics_by_State/Delaware/Publications/DE%20Ag%20Brochure_web.pdf (accessed 12 August 2016).

[24] Massey MS, Davis JG, Sheffield RE, Ippolito JA. 2007. Struvite production from dairy wastewater and its potential as a fertilizer for organic production in calcareous soils. In: International Symposium on Air Quality and Waste Management for Agriculture. CD-Rom Proceedings of the 16–19 September 2007, Conference (Broomfield, Colorado), USA. ASABE Publication Number 701P0907cd.

[25] Sharpley AN, Herron S, Daniel T. Overcoming the challenges of phosphorous-based management in poultry farming. Journal of Soil Water Conservation 2007; 62:375–389.

[26] USEPA. 2001. Ambient Water Quality Criteria Recommendations—Information Supporting the Development of State and Tribal Nutrient Criteria—Rivers and Streams in Nutrient Ecoregion XIV: Report EPA 822B-00-022. p. 84.

[27] Schindler DW. Eutrophication recovery in experimental lakes: implications for lake management. Science 1974; 184(4139):897–899. doi: 10.1126/science.184.4139.897.

[28] Schindler DW. Evolution of phosphorus limitation in lakes. Science 1977; 195(4275):260–262. doi: 10.1126/science.195.4275.260.

[29] Havens KE. Cyanobacteria blooms: effects on aquatic ecosystems. Advances in Experimental Medicine and Biology 2008; 619:733–747.

[30] Anderson DM, Glibert PM, Burkholder JM. Harmful algal blooms and eutrophication: nutrient sources, composition, and consequences. Estuaries 2002; 25:704–726.

[31] Peterson BJ, Hobbie JE, Hershey AE, Lock MA, Ford TE, Vestal JR, McKinley VL, Hullar MAJ, Miller MC, Ventullo RM, Volk GS. Transformation of a Tundra river from heterotrophy to autotrophy by addition of phosphorous. Science 1985; 229:1383–1386.

[32] Ozbay G, Roeske K, Chintapenta LK, Kalavacharla V, Stone M, Phalen L. Land use impacts: the effects of non-native grasses on marsh and aquatic ecosystem. Ecosystems and Ecography 2014; 4:1–5. http://dx.doi.org/10.4172/2157-7625.1000151.

[33] Able KW, Hagan SM. Effects of common reed (*Phragmites australis*) invasion on marsh surface macrofauna: response of fishes and decapod crustaceans. Estuaries 2000; 23: 633–646.

[34] Hunter KL, Fox DA, Brown LM, Able KW. Responses of resident marsh fishes to stages of *Phragmites australis* invasion in three mid Atlantic estuaries. Estuaries and Coasts 2006; 29: 487–498.

[35] Jivoff PR, Able KW. English Title: Blue crab, *Callinectes sapidus*, response to the invasive common reed, *Phragmites australis*: abundance, size, sex ratio, and molting frequency. Estuaries 2003; 26: 587–595.

[36] Seliskar DM, Smart KE, Higashikubo BT, Gallagher JL. Seedling sulfide sensitivity among plant species colonizing Phragmites infested wetlands. Wetlands 2004; 24: 426–433.

[37] Seliskar DM. 2008. Phragmites australis: A Closer Look at a Marsh Invader. http://www1.udel.edu/PR/UDaily/2008/oct/PhragmitesBulletin.pdf (accessed 15 June 2016).

[38] DNERR. 2005. Delaware Estuarine Research Reserve Management Plan. https://coast.noaa.gov/data/docs/nerrs/Reserves_DEL_MgmtPlan.pdf. p. 124 (accessed 18 June 2016).

[39] DNREC. 2005. Delaware Bay and Estuary Whole Basin Assessment Report. Delaware Department of Natural Resources and Environmental Control Document Number 40-01-01/05/02/01, Dover, USA.

[40] State of Delaware 1994. Statewide Wetland Mapping Project (SWMP). Prepared for the State of Delaware's Department of Natural Resources and Environmental Control (DNREC) and for the Department of Transportation (DELDOT), Dover, USA.

[41] Tiner RW. 2001. Delaware's Wetlands: Status and Recent Trends. U.S. Fish and Wildlife Service, Cooperative National Wetlands Inventory Publication, Northeast Region, Hadley, Massachusetts, USA.

[42] Rogerson A, Jacobs A, Howard A. 2010. Condition of Wetlands in the St. Jones River Watershed. January 2010. St. Jones River Watershed Report. Final report submitted to U.S. Environmental Protection Agency Region III for Assistance # WL-97329901-0 to the Delaware Department of Natural Resources and Environmental Control, Water Resources Division/Watershed Assessment Section Dover, Delaware 19904. p. 79.

[43] Harding LW Jr, Perry E. Long-term increase of phytoplankton biomass in Chesapeake Bay. Marine Ecology Progress Series 1997; 157:39–52.

[44] Nixon SW, Oviatt CA, Frithsen J, Sullivan B. Nutrients and the productivity of estuarine and coastal marine systems. Journal of the Limnological Society of Southern Africa 1986; 12:43–71.

[45] Harding LW Jr. Mallonee ME, Perry ES. 2013. Long-term trend analysis of chlorophyll in Chesapeake Bay using shipboard and aircraft observations. Marine Ecology Progress Series (in preparation).

[46] PACD. 2009. PA Chesapeake Bay Education Office. http://pacd.org/education/chesapeake-bay-education-office/ (accessed 20 July 2016).

[47] Chesapeake Bay Foundation Report. 2016. What is Killing the Bay? http://www.cbf.org/how-we-save-the-bay/chesapeake-clean-water-blueprint/what-is-killing-the-bay#continued (accessed 20 July 2016).

[48] The PEW Environment Group. 2011. Big Chicken. Pollution and Industrial Poultry Production in America. Washington, DC. 2004. p. 36. http://www.pewtrusts.org/~/media/legacy/uploadedfiles/peg/publications/report/pegbigchickenjuly2011pdf.pdf (accessed 15 June 2016).

[49] Ogejo JA. 2009. Selecting a Treatment Technology for Manure Management. Virginia Cooperative Extension, Virginia Tech. Publication 442–306.

[50] Chesapeake Bay Program. 2007. The Chesapeake Bay Watershed. http://www.chesapeakebay.net/discover/baywatershed (accessed 15 June 2016).

[51] Atallah L, Lo B, Yang G. Can pervasive sensing address current challenges in global healthcare? Journal of Epidemiology and Global Health 2012; 2(1):1–13. doi:10.1016/j.jegh.2011.11.005.

[52] NOAA National Ocean Service. 2015. What is Remote Sensing? http://oceanservice.noaa.gov/facts/remotesensing.html (accessed 15 June 2016).

[53] USGS. 2016. Land Remote Sensing Program. http://remotesensing.usgs.gov/%5C/gallery/gallerynojs.php?id=399&cat=8 (accessed 15 June 2016).

[54] Fan C, Glibert PM, Burkholder JM. Characterization of the affinity for nitrogen, uptake kinetics, and environmental relationships for *Prorocentrum minimum* in natural blooms and laboratory cultures. Harmful Algae 2003; 2(4): 283–299.

[55] Anderson DM, Burkholder JM, Cochlan WP, Glibert PM, Gobler CJ, Heil CA, Kudela RM, Parsons ML, Rensel JEJ, Townsend DW, Trainer VL, Vargo GA. Harmful algal blooms and eutrophication: examining linkages from selected coastal regions of the United States. Harmful Algae 2008; 8(1): 39–53.

[56] Fourqurean JW, Jones RD, Zieman JC. Process influencing water column nutrient characteristics and phosphorus limitation of phytoplankton biomass in Florida Bay, FL, USA: inferences from spatial distributions. Estuarine, Coastal and Shelf Science 1993; 36(3):295–314.

[57] Kendrick P. Remote sensing and water quality. Journal Water Pollution Control Federation 1976; 48(10): 2243–2246.

[58] Brando VE, Dekker AG. 2003. Satellite hyperspectral remote sensing for estimating estuarine and coastal water quality. IEEE Transactions on Geoscience and Remote Sensing 2003; 41(6): 1378–1387.

[59] Campbell G, Phinn SR, Dekker AG, Brando V E. Remote sensing of water quality in an Australian tropical freshwater impoundment using matrix inversion and MERIS images. Remote Sensing of Environment 2011; 115(9): 2402–2414.

[60] Mustard JF, Sunshine JM. 1999. Spectral analysis for Earth science: investigation using remote sensing data. In: Rencz, A.N. (Ed.), Remote Sensing for the Earth Science: Manual of Remote Sensing, Volume 3, 3rd Edition. Wiley, New York, NY, USA.

[61] GIS Geography. 2016. Multispectral vs Hyperspectral Imagery Explained. http://gisgeography.com/multispectral-vs-hyperspectral-imagery-explained/ (accessed 15 June 2016).

[62] Fisher R, Perkins S, Walker A, Wolfart E. 2003. Multi-Spectral Images. http://homepages.inf.ed.ac.uk/rbf/HIPR2/mulimage.htm (accessed 20 May 2016).

[63] Elhadi A, Mutanga O, Rugege D. Multispectral and hyperspectral remote sensing for identification and mapping of wetland vegetation: a review. Wetlands Ecology and Management 2010; 18: 281–296.

[64] Shippert P. 2012. Introduction to Hyperspectral Image Analysis. Research Systems. Ohio Space Journal. p. 13. http://spacejournal.ohio.edu/pdf/shippert.pdf (accessed 20 May 2016).

[65] Artigas F, Pechmann IC. Balloon imagery verification of remotely sensed *Phragmites australis* expansion in an urban estuary of New Jersey, USA. Landscape and Urban Planning 2010; 95: 105–112.

[66] Bukata, RP, Jerome JH, Kondratyev KY, Pozdnyakov DV. 1995. Optical Properties and Remote Sensing of Inland and Coastal Waters. CRC Press, Taylor and Francis Group, Boca Raton, FL, USA. p. 368.

[67] Chang GK, Mahoney A, Briggs-Whitmire DK, Mobley C, Lewis M, Moline M, Boss E, Kim M, Philpot W, Dickey T. The new age of hyperspectral oceanography. Oceanography 2004; 17(2): 16–23.

[68] Nair RR, Blake P, Grigorenko AN, Novoselov KS, Booth TJ, Stauber T, Peres NMR, Geim AK. Fine structure constant defines visual transparency of graphene. Science 2008; 320(5881):1308–1308. ISSN 0036-8075.

[69] Louchard EM, Reid RP, Stephens FC, Davis CO, Leathers RA, Downes TV. Optical remote sensing of benthic habitats and bathymetry in coastal environments at Lee Stocking Island, Bahamas: a comparative spectral classification approach. Journal of Limnology and Oceanography 2003; 48(1–2): 511–521. The American Society of Limnology and Oceanography, Inc.

[70] Althuis IJA. Suspended particulate matter detection in the North Sea by hyperspectral airborne remote sensing. Aquatic Ecology 1998; 32: 93–98.

[71] Tsai F, Philpot W. Derivative analysis of hyperspectral data. Remote Sensing of Environment 1998; 66:41–51.

[72] Ruffin C, King RL, Younan NH. A combined derivative spectroscopy and Savitzky-Golay filtering method for the analysis of hyperspectral data. GIScience and Remote Sensing 2008; 45 (1):1–15.

[73] Senay GB, Shafique NA, Autrey BC, Fulk F, Cormier SM. The selection of narrow wavebands for optimizing water quality monitoring on the Great Miami River, Ohio using hyperspectral remote sensor data. Journal of Spatial Hydrology 2002; 1(1):1–24.

[74] Hunter PD, Tyler AN, Carvalho L, Codd GA, Maberly SC. Hyperspectral remote sensing of cyanobacterial pigments as indicators for cell populations and toxins in eutrophic lakes. Remote Sensing of Environment 2010; 114(11): 2705–2718.

[75] Jo Y-H, Oliver MJ, Ozbay G. Estimating distributions of biogeochemical constituents using hyperspectral remote sensing in Delaware Bay. Delaware EPSCOR Seed Grant Program 2011–2012. Focal Area: Theme 3: Environmental Observation and Sensing. p. 17.

[76] Jo Y-H, Yan XH. 2011. Integrated altitude-adjustable remote sensing systems and methods, Patent Number, UOD-382USP (in pending).

[77] Vitousek PM, Mooney HA, Lubchenco J, Melillo JM. Human domination of Earth's ecosystems. Science 1997; 277(5325):494–499. doi: 10.1126/science.277.5325.494.

[78] Matson PA, Parton WJ, Power AG, Swift MJ. Agricultural intensification and ecosystem properties. Science 1997; 277(5325):504–509. doi: 10.1126/science.277.5325.504.

[79] Lotze HK, Lenihan HS, Bourque BJ, Bradbury RH, Cooke RG, Key MC, Kidwell SM, Kirby MX, Peterson CH, Jackson JB. Depletion, degradation, recovery potential of estuaries and coastal seas. Science 2006; 312 (1806). doi: 10.1126/science.1128035.

[80] Fondriest Environmental Inc. 2016. Turbidity, Total Suspended Solids & Water Clarity. http://www.fondriest.com/environmental-measurements/parameters/water-quality/turbidity-total-suspended-solids-water-clarity/

[81] Davies-Colley RJ, Smith DG. Turbidity, suspended sediment, and water clarity: a review. Journal of the American Water Resources Association 2001; 37:1085–1101.

[82] Cloern J. Turbidity as a control on phytoplankton biomass and productivity in estuaries. Continental Shelf Research 1987; 7:1367–1381.

[83] De Robertis A, Ryer CH, Veloza A, Brodeur RD. Differential effects of turbidity on prey consumption of piscivorous and planktivorous fish. Canadian Journal of Fish and Aquatic Sciences 2003; 60:1517–1526.

[84] Utne-Palm AC. Visual feeding of fish in a turbid environment: physical and behavioural aspects. Marine and Freshwater Behavior and Physiology 2001; 35:111–128.

[85] Pennock JR, Sharp JH. Phytoplankton production in the Delaware estuary: temporal and spatial variability. Marine Ecology Progress Series 1986; 34:143–155.

[86] Kirk JTO. 1994. Light and Photosynthesis in Aquatic Ecosystems: 2nd Edition. Cambridge University Press: New York City, NY, USA. p. 509.

[87] Olli G, Darracq A, Destouni G. Field study of phosphorous transport and retention in drainage reaches. Journal of Hydrology 2009; 365:46–55.

[88] Correll D. The role of phosphorous in the eutrophication of receiving waters: a review. Journal of Environmental Quality 1998; 27:261–267.

[89] Reddy KR, Admas JF, Richardson C. Potential technologies for remediation of Brownfield. Practice Periodical of Hazardous Toxic and Radioactive Waste Management 1999; 3:61–68.

[90] Conley DJ. Biogeochemical nutrient cycles and nutrient management strategies. Hydrobiologia 2000; 410:87–96.

[91] RMB Environmental Laboratories Inc. 2016. Chlorophyll-*a*. http://rmbel.info/chlorophyll-a/ (accessed 15 June 2016).

[92] Gallina N, Anneville O, Beniston M. Impacts of extreme air temperatures on cyanobacteria in five deep peri-Alpine lakes. Journal of Limnology 2011; 70(2): 186–196. DOI: 10.3274/JL11-70-2-04.

[93] Ritchie JC, Cooper CM. 2001. Remote Sensing Techniques for Determining Water Quality: Applications to TMDLS, USDA, Water Environment Federation.

[94] Fondriest Environmental Inc. 2016. Chlorophyll. http://www.fondriest.com/science-library/water-quality/chlorophyll (accessed 15 June 2016).

[95] Behrenfeld M, Boss E, Siegel D, Shea D. Biospheric primary production during an ENSO transition. Science 2001; 291, 2594–2597.

[96] Lillesand TM, Kiefer RW. 1994. Remote Sensing and Image Interpretation. New York, NY: Wiley and Sons.

[97] Clark D. 1981. Phytoplankton algorithms for the Nimbus-7 CZCS; In Gower, R. (Ed.) Oceanography from Space, Plenum Press, New York, NY, p. 227.

[98] Stumpf RP, Culver ME, Tester PA, Tomlinson M, Kirkpatrick GJ, Pederson BA, Truby E, Ransibrahmanakul V, Soracco M. Monitoring *Karenia brevis* blooms in the Gulf of Mexico using satellite ocean color imagery and other data. Harmful Algae 2003; 2:147–160.

[99] Glibert PM, Magnien R, Lomas MW, Alexander J, Fan C, Haramoto E, Trice M, Kana TM. Harmful algal blooms in the Chesapeake and coastal Bays of Maryland, USA: comparison of 1997, 1998, and 1999 events. Estuaries 2001; 24: 875–883.

[100] Ritchie JC, Seyfried MS, Chopping MJ, Pachepsky Y. Airborne laser technology for measuring rangeland conditions, Journal of Range Management 2001; 54(suppl):A8–A21.

[101] Roeske K. 2013. Assessing the impact of *Phragmites australis* subspecies Australis on blue crab (*Callinectes sapidus*) and fish population dynamics in Blackbird Creek, Delaware. Master's Thesis. Natural Resources Program. Department of Agriculture and Natural Resources, Delaware State University, Dover, DE, USA. p 230.

[102] Friends of the Earth Europe. 2013. The Environmental Impacts of Glyphosate. http://www.foeeurope.org/sites/default/files/press_releases /foee_5_environmental_impacts_glyphosate.pdf> (accessed 15 June 2016).

[103] Fish and Wildlife Service. 2004. Comprehensive Conservation Plan. Accessed at <http://www.fws.gov/mountain-prairie/planning /ccp/ut/fhs/documents /fhs_2004_ccpdraft_4consequences.pdf > (accessed 20 May 2016).

[104] Lowery TA, Tate LG. Effect of hypoxia on hemolymph lactate and behavior of the blue crab *Callinectes sapidus* Rathbun in the laboratory and field. Comparative Biochemistry and Physiology, Part A. 1986; 85: 689–692.

[105] Talke SA, Stacey MT. Suspended sediment fluxes at an intertidal flat: the shifting influence of wave, wind, tidal, and freshwater forcing. Continental Shelf Research 2007; 28: 710–725.

[106] Wischmeier WH, Smith DD. 1978. Predicting Rainfall Erosion Losses—A Guide to Conservation Planning. USDA, Science and Education Administration, Hyattsville, MD, USA. p. 62.

[107] Steele JH, Henderson EW. The role of predation in plankton models. Journal of Plankton Research 1992; 14: 157–172.

[108] Perissinotto R, Pillay D, Bate G. Microalgal biomass in the St. Lucia Estuary during the 2004–2007 drought period. Marine Ecology Progress Series 2010; 405: 147–161.

[109] Carpenter SR, Caraco NF, Correll DL, Howarth RW, Sharpley AN, Smith VH. Nonpoint pollution of surface waters with phosphorus and nitrogen. Ecological Applications Journal 1998; 8: 559–568.

[110] Bennett EM, Carpenter SR, Caraco NF. Human impact on erodible phosphorus and eutrophication: a global perspective. Bioscience 2001; 51: 227–234.

[111] Davis RL, Zhang H, Schroder JL, Wang JJ, Payton ME, Zazulak A. Soil characteristics and phosphorus loss in runoff. Journal of Environmental Quality 2005; 34: 1640–1650.

[112] Holliday CP, Rasmussen TC, Miller WP. 2003. Establishing the relationship between turbidity and total suspended sediment concentration. Proceedings of the 2003 Georgia Water Resources Conference.

[113] Wall GJ, Bos AW, Marshall AH. The relationship between phosphorous and suspended sediment loads in Ontario watersheds. Journal of Soil Water Conservation 1996; 51: 504–507.

[114] Dahl TE. 1990. Wetlands Loss Since the Revolution. Wetland Losses in the United States 1780s to 1980s. National Wetlands Inventory. U.S. Fish and Wildlife Service, 9720 Executive Center Drive, Suite 101, Monroe Building, St. Petersburg, FL, USA.

[115] Smith LED, Siciliano G. A comprehensive review of constraints to improved management of fertilizers in China and mitigation of diffuse water pollution from agriculture. Agriculture, Ecosystems and Environment 2015; 209: 15–25. doi:10.1016/j.agee.2015.02.016.

[116] Salem F, Ozbay G, Roper W. Identification of Suspended Sediments and Chlorophyll-a in the Blackbird Creek, Delaware Using AISA Hyperspectral Data and Analysis. Delaware State University, Department of Agriculture and Natural Resources, Dover, DE, USA. Unpublished Report for the USDA-NIFA CBG Grant Award# 2010-38821-21454. p23.

[117] Shafique NA, Fulk F, Autrey BC, Flotemersch J. Hyperspectral Remote Sensing of Water Quality Parameters for Large Rivers in the Ohio River Basin. ICRW Proceedings 2001; pp. 216–221. http://www.tucson.ars.ag.gov/icrw/proceedings/shafique.pdf (accessed 15 June 2016).

[118] Agawin SR, Duarte CM, Agustı S. Nutrient and temperature control of the contribution of picoplankton to phytoplankton biomass and production. By the American Society of Limnology and Oceanography, Inc., Limnology and Oceanography Journal 2000; 45(3): 591–600.

[119] Ritchie JC, Zimba PV, Everitt JH. 1976. Remote sensing techniques to assess water quality. Photogrammetric Engineering and Remote Sensing 03-907. p. 37. ftp://hrsl.ba.ars.usda.gov/pub/incoming/RSinARS/white_papers/03-907a.pdf. Retrieved by June 15, 2016.

[120] Härmä P, Vepsäläinen J, Hannonen T, Pyhälahti T, Kämäri J, Kallio K, Eloheimo K, Koponen S. Detection of water quality using simulated satellite data and semi-empirical algorithms in Finland. The Science of Total Environment 2001; 268(1–3):107–121.

[121] Ammenberg J, Hjelm O, Quotes P. The connection between environmental management systems and continual environmental performance improvements. Corporate Environmental Strategy 2002; 9:183–192.

[122] Ansotegui A, Sarobe A, Trigueros JM, Urrutxurtu I, Orive E. Size distribution of algal pigments and phytoplankton assemblages in a coastal estuarine environment: contribution of small eukaryotic algae, Journal of Plankton Research 2003; 25(4):341–355.

[123] Turner JT, Tester PA. Toxic marine phytoplankton, zooplankton grazers, and pelagic food webs. Part 2: The Ecology and Oceanography of Harmful Algal Blooms. Limnology and Oceanography. 1997; 42 (5): 1203–1214.

[124] Tester PA, Stumpf RP, Vukovich FM, Fowler PK, Turner JT. An expatriate red tide bloom: transport, distribution, and persistence. Limnology and Oceanography 1991; 36:1953–1961.

[125] Keafer BA, Anderson DM. 1993, Use of remotely-sensed sea surface temperatures in studies of *Alexandrium tamarense* bloom dynamics. In Toxic Phytoplankton in the Sea, Proceedings of 5th International Conference. Smayda TM and Shimizu Y. (Ed.), Elsevier, Amsterdam. pp. 763–768.

[126] Hovis WA. Nimbus-7 Coastal Zone Color Scanner system description and initial imagery. Science 1980; 210: 60–63.

[127] Feldman GC, Kuring N, Ng C, Esaias W, McClain C, Elrod J, Maynard N, Endres D, Evans R, Brown J, Walsh S, Carle M, Podesta G. 1989. Ocean color: availability of the global data set. Eos Trans. AGU, 70, 640.

[128] IOCCG. 1999. Status and plans for satellite ocean colour mission: considerations for complementary missions", In Yoder J. (Ed.), Reports of the International Ocean Colour Coordinating Group, Number 2 IOCCG, Dartmouth, N.S., Canada.

[129] Antoine D, Morel A, Gentili B, Gordon H, Banzon V, Evans R, Brown J, Walsh S, Baringer W, Li A. In search of long-term trends in ocean color. Eos 2003; 84(32) 301: 308–309.

[130] Smith RC, Baker KS. Oceanic chlorophyll concentrations as determined by satellite (Nimbus-7 Coastal Zone Color Scanner). Marine Biology 1982; 66:269–279.

[131] Mantoura RFC, Llewellyn CA. The rapid determination of algal chlorophyll and carotenoid pigments and their breakdown products in natural waters by reverse-phase high performance liquid chromatography. Analytica Chimica Acta 1983; 151:297–314.

[132] Gieskes WW. 1991. Algal pigment fingerprints: clue to taxon specific abundance, productivity, and degradation of phytoplankton in seas and oceans. In Demers S (Ed.), Particle Analysis in Oceanography. NATO ASI Series. Vol. G27 Springer-Verlag, Berlin. pp. 61–99.

[133] Millie DF, Paerl HW, Hurley JP, Kirkpatrick GJ. Microalgal pigment assessments using high performance liquid chromatography: a synopsis of organismal and ecological applications. Canadian Journal of Fisheries and Aquatic Science 1993; 50:2513–2527.

[134] Morel A, Prieur L. Analysis of variation in ocean color. Limnology and Oceanography Journal 1997; 22: 709–722.

[135] Darecki M, Weeks A, Sagan S, Kowalczuk P, Kaczmarek S. Optical characteristics of two contrasting case 2 waters and their influence on remote sensing algorithms. Continental Shelf Research 2003; 23(3–4): 237–250.

[136] Davis CO, Bowles J, Leathers RA, Korwan D, Downes T V, Snyder WA, Rhea WJ, Chen W, Fisher J, Bissett WP, Reisse RA. Ocean PHILLS 18 hyperspectral imager: design, characterization, and calibration. Optics Express 2002; 10(4): 210–221.

[137] Chang GC, Mahoney K, Briggs-Whitmire A, Kohler D, Mobley C, Lewis M, Moline M, Boss E, Kim M, Philpot W, Dickey T. The new age of hyperspectral oceanography. Oceanography 2004; 17(2): 22–29.

[138] Johnsen G, Nelson NB, Jovine RVM, Prezelin BB. Chromoprotein and pigment dependent modeling of spectral light absorption in two dinoflagellates, *Prorocentrum minimum* and *Heterocapsa pygmaea*. Marine Ecology Progress Series 1994; 114: 245–258.

[139] Tester PA, Geesey ME, Guo C, Paerl HW, Millie DF. Evaluating photoplankton dynamics in the Newport River estuary (North Carolina) by HPLC derived pigment profiles. Marine Ecology Progress Series 1995; 124: 237–245.

[140] Millie DF, Schofield OM, Kirkpatrick GJ, Johnson G, Tester PA, Vinyard BT. Detection of harmful algal blooms using photopigments and absorption signatures: a case study of the Florida red tide dinoflagellate, *Gymnodium breve*. Limnology and Oceanography 1997; 42(5): 1240–1251.

[141] Schofield O, Arnone R, Bissett W, Dickey T, Davis C, Finkel Z, Oliver M, Moline M. Watercolors in the coastal zone: What can we see? Oceanography 2004; 17(2): 24–31.

[142] Schofield O, Bergmann T, Oliver M, Irwin A, Kirkpatrick G, Bissett W, Moline M, Orrico C. Inversion of spectral absorption in the optically complex coastal waters of the Mid-Atlantic Bight. Journal of Geophysical Research 2004; 109, C12S04. doi:10.1029/2003JC002071.

[143] Richardson LL, Kruse FA. 1999. Identification and classification of mixed phytoplankton assemblages using AVIRIS image-derived spectra. AVIRIS Workshop, Pasadena, CA, USA.

[144] Richardson LL, Kruse FA. 2000. Use of AVIRIS spectral data to discriminate mixed phytoplankton communities, seagrass beds, and benthic algal mats in Florida Bay, USA. AVIRIS Workshop, Pasadena, CA, USA.

[145] Glenn S, Schofield O. Observing the oceans from the COOL room: our history, experience, and opinions. Oceanography 2003; 16(4): 37–52.

[146] Schofield O, Grzymski J, Bissett WP, Kirkpatrick GJ, Millie DF, Moline M, Roesler CS. Optical monitoring and forecasting systems for harmful algal blooms: possibility or pipe dream? Journal of Phycology 1999; 35: 1477–1496.

[147] Fan C, Warner RA. Characterization of water reflectance spectra variability: implications for hyperspectral remote sensing in estuarine waters. Marine Science 2014; 4(1): 1–9.

[148] O'Reilly JE, Maritorena S, Mitchell BG, Siegel DA, Carder KL, Garver SA, Kahru M, McClain C. Ocean color chlorophyll algorithms for SeaWiFS. Journal of Geophysical Research 1998; 103: 24,937–24,953.

[149] Warner RA, Fan C. Optical spectra of phytoplankton cultures for remote sensing applications: focus on harmful algal blooms. International Journal of Environmental Science and Development 2013, 4(2); 94–98.

[150] Fan C. Spectral analysis of water reflectance for hyperspectral remote sensing of water quailty in estuarine water. Journal of Geoscience and Environment Protection 2014; 2(2): 19–27. s. http://www.scirp.org/journal/gep http://dx.doi.org/10.4236/gep.2014.22004.

[151] Olmanson LG, Brezonik PL, Bauer ME. Airborne hyperspectral remote sensing to assess spatial distribution of water quality characteristics in large rivers: the Mississippi River and its tributaries in Minnesota. Remote Sensing of Environment 2013; 130(0): 254–265.

[152] Toole DA, Siegel DA. 2001. Modes and mechanisms of ocean color variability in the Santa Barbara Channel. Journal of Geophysical Research: Oceans (1978–2012); 106(C11): 26985–27000.

[153] Lubac B, Loisel H. Variability and classification of remote sensing reflectance spectra in the eastern English Channel and southern North Sea. Remote Sensing of Environment 2007; 110(1): 45–58.

[154] Legleiter CJ, Roberts DA. Effects of channel morphology and sensor spatial resolution on image-derived depth estimates. Remote Sensing of Environment 2005; 95(2): 231–247.

[155] Schalles JF. 2006. Optical remote sensing techniques to estimate phytoplankton Chlorophyll-a concentrations in coastal. In Richardson LL, LeDrew EF (Eds.), Remote Sensing of Aquatic Coastal Ecosystem Processes, Science and Management Applications. Springer. Volume 9, pp. 27–79.

[156] Doxaran D, Cherukuru R, Lavender S. Use of reflectance band ratios to estimate suspended and dissolved matter concentrations in estuarine waters. International Journal of Remote Sensing 2005; 26(8): 1763–1769.

[157] DNERR. 1999. Delaware National Estuarine Research Reserve (DNERR) Estuarine Profile. p. 158. http://www.dnrec.delaware.gov/coastal/DNERR/Documents/Estuarine%20Profile%201999.pdf (accessed 15 June 2016).

[158] Yang Z, Reiter M. Land use/cover changes within riparian buffers in the State of Delaware. JEMREST 2008; 4: 39–52.

[159] Gitelson A. 1992.The peak near 700 nm on reflectance spectra of algae and water: relationships of its magnitude and position with chlorophyll concentration. International Journal of Remote Sensing 1992; 13: 3367–3373.

[160] Gitelson A. The nature of the peak near 700 nm on the radiance spectra and its application for remote estimation of phytoplankton pigments in inland waters, Optical Engineering and Remote Sensing, SPIE 1993; 1971: 170–179.